Chapter 8 –

Light microscopic study of the histological morphology of the liver and kidney to determine the effects of aspartame

RESEARCH QUESTION 6:

How does aspartame affect the normal histological morphology of the liver and kidney?

8.1 INTRODUCTION

The components of blood (plasma with coagulation factors, fibrin fibres, and platelet aggregates and leukocytes) were studied during the first part of this thesis. It was found that all the constituents of the coagulation system, from the coagulation factors to the intravascular anti-coagulation system were affected by the treatment with aspartame. This being the case, the aim of this chapter of the thesis was to determine whether two of the major filtration organs in the body, namely the liver and kidneys were adversely affected by the treatment with aspartame.

Ranney and co-workers in 1976 undertook a comparative study of the metabolism of aspartame in experimental animals and humans. The metabolism of aspartame was studied in mice, rats, rabbits, dogs, monkeys and humans. Ranney and co-workers found that the compound was digested in all species in the same way as are natural constituents of the diet. Hydrolysis of the methyl group by internal esterases yielded methanol, which was oxidized in the one-carbon metabolic pool of carbon dioxide (CO_2). The resultant dipeptide was split at the mucosal surface by dipeptidases and the free amino acids were absorbed. The aspartic acid moiety was transformed in large part to CO_2 through its entry into the tricarboxylic acid cycle. Phenylalanine was primarily incorporated into body protein either unchanged or as its major metabolite, tyrosine.

Adult male rats were given an oral dose of 10mg/kg aspartame 14C-labelled in the methanol carbon. At times intervals of up to 6 hours, the radioactivity in the plasma and several organs was investigated. Most of the radioactivity found (0.98% in plasma, 0.75% in liver) was bound to protein. Label present in the liver, plasma and kidney was in the range of 1-2% of the total radioactivity administered per g or ml, changing little with time. Other organs (brown and white adipose tissue, muscle, brain, cornea and retina) contained levels of label in the range of 1/12 to 1/10th of that of the liver. In all, the rat retained, 6 hours after administration about 5% label, half

of it in the liver. The specific radioactivity of the tissue protein, RNA and DNA was quite uniform. The protein label was concentrated in amino acids, different from methionine, and largely coincident with the result of protein exposure to labelled formaldehyde. DNA radioactivity was essentially in a single different adduct base, different from the normal bases present in DNA. The nature of the tissue label accumulated was, thus, a direct consequence of formaldehyde binding to tissue structures. The administration of labelled aspartame to a group of cirrhotic rats resulted in comparable label retention by tissue components, which suggests that liver function (or its defect) has little effect on formaldehyde formation from aspartame and binding to biological components. The chronic treatment of a series of rats with 200 mg/kg of non-labelled aspartame during 10 days resulted in the accumulation of even more label when given the radioactive bolus, suggesting that the amount of formaldehyde adducts coming from aspartame in tissue proteins and nucleic acids may be accumulative. It was concluded that aspartame consumption may constitute a hazard because of its contribution to the formation of formaldehyde adducts (Trocho *et al.*, 1998).

The renal cells were visualized by means of three-dimensional NaOH maceration. The three-dimensional fine structure of the cells composing the renal tissue was demonstrated by SEM after removal of extracellular matrices by NaOH maceration. Takahashi-Iwanaga (1992) focussed on glomerular mesangial cells, extraglomerular mesangial cells, and epithelial cells in the thin limb's of Henle's loop in the rat, rabbit and dog. Mesangial cells revealed a rough surface covered by short microvilli. The cells extended long branching processes in close association with the glomerular capillary, suggesting a role for them of regulating the capillary calibre. The mesangial cells interdigitated with each other by means of their microvilli, forming an intercellular labyrinth. Extraglomerular mesangial cells at the glomerular hilus were also covered with microvilli, which forms narrow labyrinthine spaces between the cells. The labyrinth among the mesangial cells and that among the extraglomerular mesangial cells connected with each other at the hilus, giving rise to a channel system leading from the periphery of the glomerulus through the hilus to the interstitial space outside the glomerulus. Renal tubule cells displayed complicated intra- and intercellular interdigitations on the basal aspect. The pattern of epithelial interdigitations was specific to each tubular segment. The descending and ascending thin limbs of the long loops demonstrated a striking contrast to each other. The former was characterized by moderate intercellular interdigitation and by numerous microvilli on the lateral

and basal surfaces; the latter was marked by elaborate, pectineal interdigitations, and by smooth basolateral surfaces (Takahashi-Iwanaga, 1992).

8.2 MATERIALS AND METHODS

8.2.1 Exposure of animals to aspartame

Rabbits in both the control and aspartame group were exposed to double distilled water and aspartame, respectively, for 25 exposures in 37 days for the three consecutive concentrations (34mg/kg; 100mg/kg and 150mg/kg aspartame). A two week resting period was allowed after completion of a concentration. Approximately one week after the last concentration was completed, the rabbits were terminated and dissected for their liver and kidney.

8.2.2 Termination of the study

After the treatment periods were completed, all the rabbits were euthanized by means of intra-peritoneal injection with sodium pentobarbitonehydrochloride (2ml) by a skilled person experienced in this technique (Mrs Annette de Freitas, animal technologist at the Medunsa campus of the University of Limpopo). All the adult rabbits not utilised for dissection were cremated. Five rabbits, 3 controls and 2 treated with aspartame (with negative/adverse clotting profiles) were dissected for the soft tissue of their livers and kidneys for light microscopic studies. After harvesting of the necessary specimens, the carcasses were cremated at the University of Limpopo, Medunsa campus.

8.2.3 Dissection and fixing of samples

Five rabbits (3 controls and 2 aspartame-treated) were given a general anaesthetic (Atravet) to make them sleepy, where-after each were euthanized by means of injection with 2ml phenobarbitone when needed for dissection. The thoracic and abdominal cavities were opened and the required organs were identified: liver and kidneys. The organs were removed and the tissue samples collected from each organ. The liver and kidney sections were fixed in 4% Formaldehyde. Tissue was obtained from the left and right lobes as well as the hilus of the liver and from the cortex and medulla of the kidney.

8.2.4 Pre-embedding procedures

After approximately a month in fixative, the tissue (liver and kidney) was removed from the fixative and serially dehydrated in 70% and 90% ethanol, followed by three changes of absolute ethanol. After dehydration, the tissue was placed in xylene (clearing agent) overnight. The tissue was then transferred into increasing concentrations of paraffin wax.

8.2.5 Embedding

Wax was melted in an embedding apparatus and the bottom of the metal embedding holders was covered with pure paraffin wax. The tissue (liver and kidney samples) was orientated and placed into the holder before complete filling with wax. The holder was covered with a plastic label, containing a record of the tissue, and allowed to set completely.

8.2.6 Sectioning

Special precautions were used to make sure that the wax blocks were of high standard before sectioning of the tissue commenced. Excess wax was trimmed away by using a scalpel. The tissue blocks, containing the liver and kidney samples was orientated and the wax block placed in the microtome for sectioning. Sections of between 5µm – 10µm (optimal 8µm) were made, and the ribbons of tissue (either liver or kidney, depending on the imbedded tissue) was transferred to a warm water bath to remove excess wax and straighten tissue sections. Sections were collected onto a glass slide and left to dry. Slides were properly labelled and numbered.

8.2.7 Approach to obtaining results from liver and kidney sections

Table 8.1: Number of views per slide for each section of tissue (liver and kidney) for each of the 5 different rabbits (3 controls and 5 aspartame treated rabbits) studied under the microscope

Tissue studied	Section of tissue	Number of sections per ribbon/slide	Number of slides	Total viewed
Liver	Left lobe	5 Serial sections	5 Slides	15 sections (Every second slide in a series with all five serial sections per slide)
	Centre of liver	5 Serial sections	5 Slides	15 sections (Every second slide in a series with all five serial sections per slide)
	Right lobe	5 Serial sections	5 Slides	15 sections (Every second slide in a series with all five serial sections per slide)
Kidney	Cortex	5 Serial sections	5 Slides	15 sections (Every second slide in a series with all five serial sections per slide)
	Medulla	5 Serial sections	5 Slides	15 sections (Every second slide in a series with all five serial sections per slide)

8.2.8 Staining with Haematoxylin and Eosin stain

Haematoxylin is a nuclear stain that stains the nuclei of the cell blue to black. The counter stain, Eosin, is responsible for the pinkish colour observed in the cytoplasm and connective tissue. Tissue were deparaffinized, rehydrated and stained with Haematoxylin for 10 minutes and counterstained in Eosin for 3 minutes. The tissue was then dehydrated and mounted for viewing under the Nikon Optiphod transmitted light microscope (Nikon Instech Co., Kanagawa, Japan).

8.3 RESULTS AND DISCUSSION

8.3.1 Microscopic study of the histological morphology of the liver

Sections from the different parts of the liver, (left lobe of liver; right lobe of liver and centre of liver) were dissected, thus it was mentioned from which part of the liver the illustration were taken, indicating possible differences and for the purpose of orientation.

Figure 8.1a and 8.1b illustrates a section through the right lobe of the liver of a control rabbit, indicating a blood vessel with hepatocytes surrounding it.

Figure 8.3a: Section through the right lobe of the liver of a control rabbit illustrating a blood vessel in the centre of the photo. Note the clear cellular membranes of the hepatocytes (black arrows) with the darker staining nuclei (circles). Dashed lines indicate polygonal shape of the hepatocytes

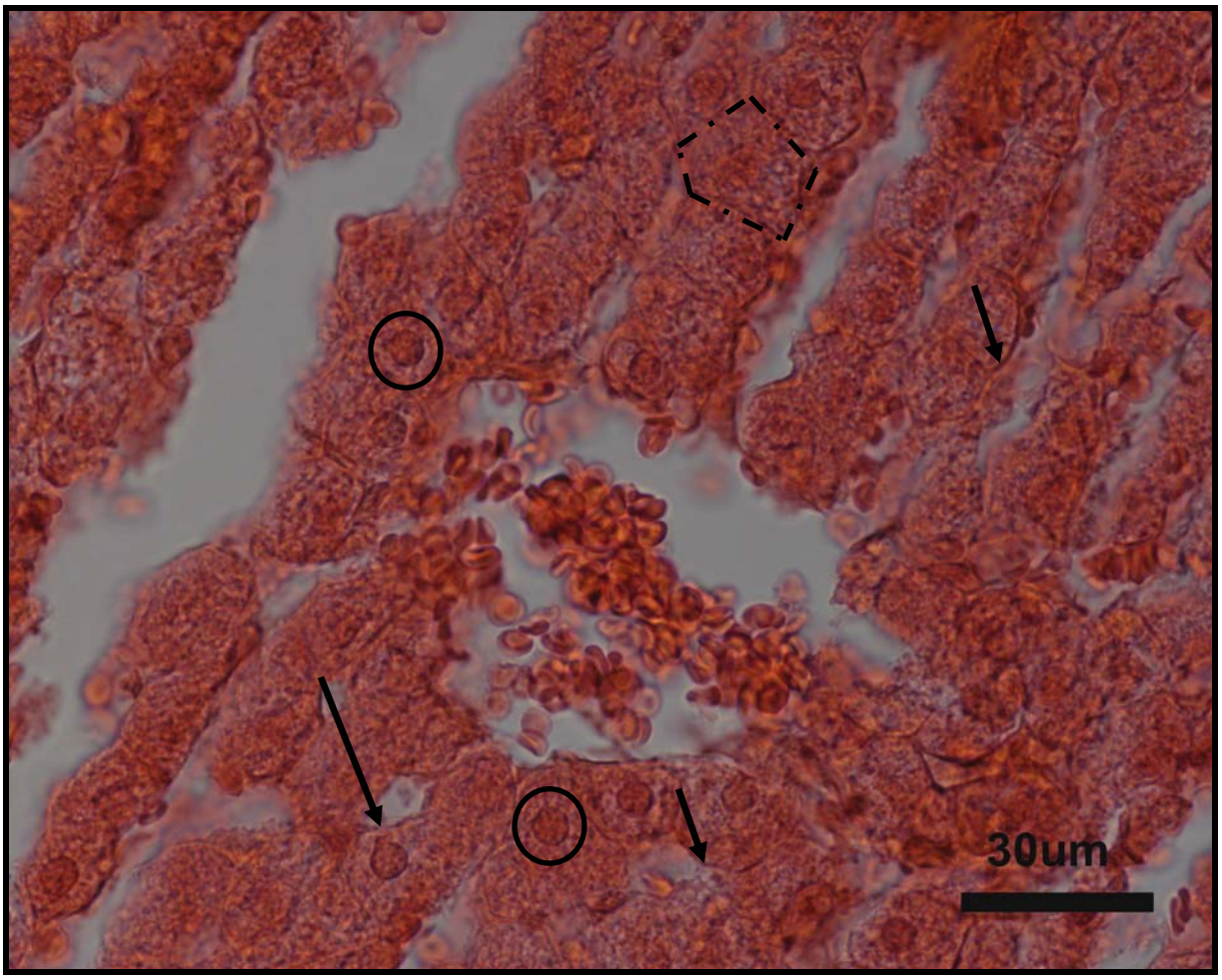

Figure 8.1b: Section through the right lobe of the liver of a control rabbit. Note the blood vessel in the centre of the photo, with two ducts. Note the clear cellular membranes of the hepatocytes (arrows) and the cuboidal epithelium lining the ducts (white arrows). Also, the endothelial lining of the blood vessel was clearly visible (dashed black arrow)

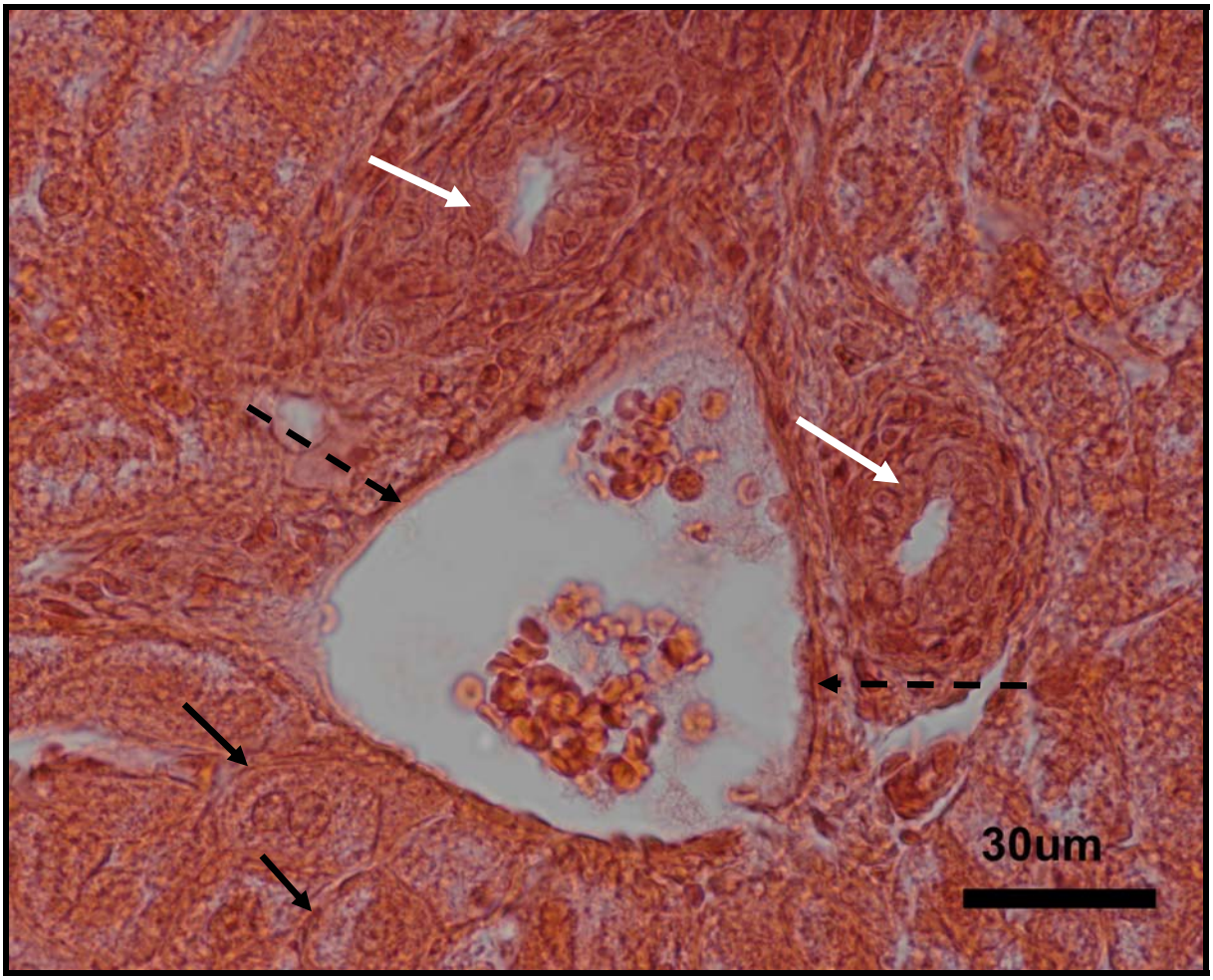

Figure 8.2 illustrates the cords of the liver, also from the right lobe, in the control rabbit.

Figure 8.4: Section through the right lobe of the liver of a control rabbit illustrating the cords that are present in the liver. Note the clear cellular membranes of the hepatocytes (arrows) and the organization of the hepatocytes in clearly distinguishable rows (dashed rectangles). Nuclei were clearly visible in the hepatocytes (circles). Endothelial lining of the blood vessel clearly visible (white arrow)

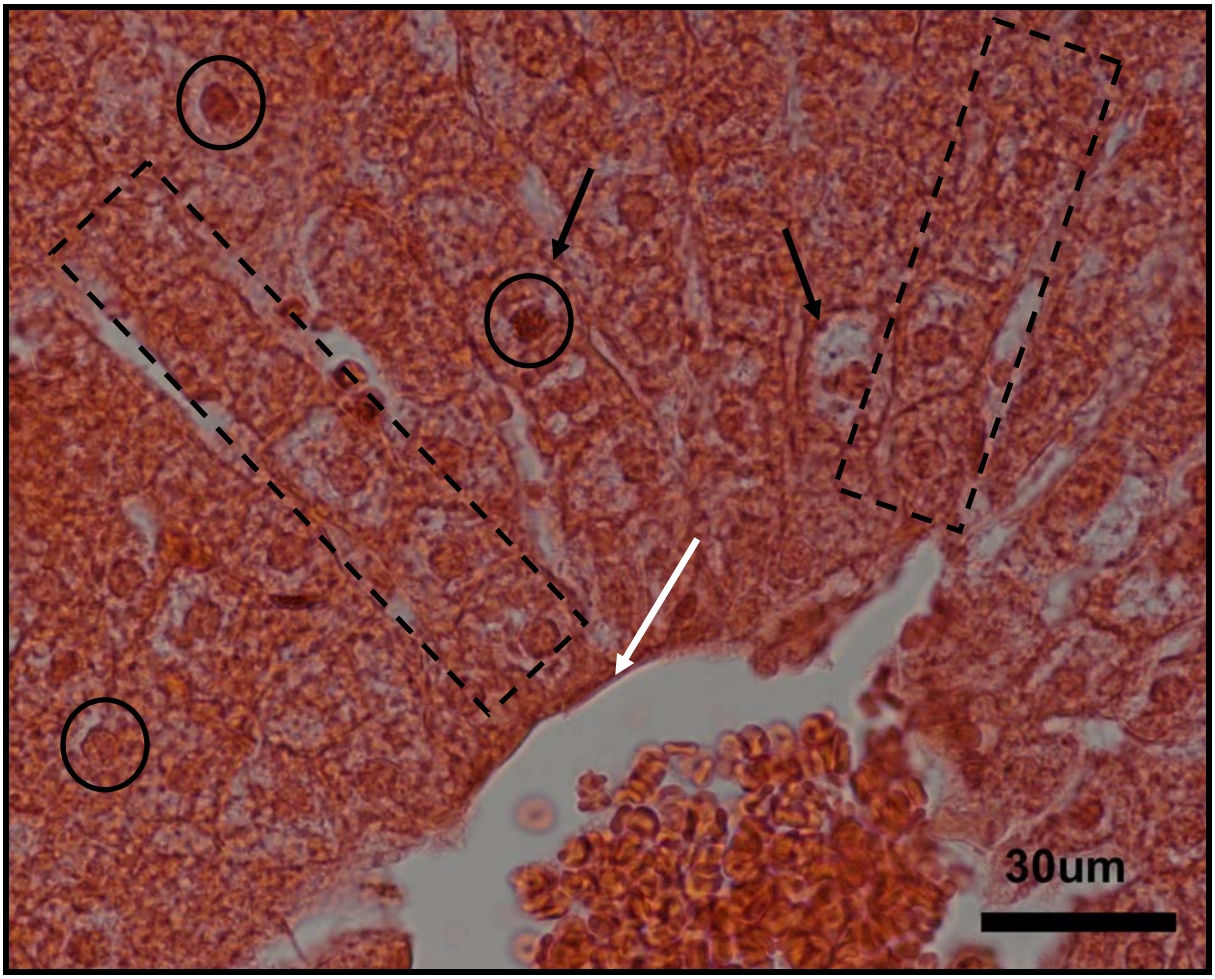

Figure 8.3a illustrates a section through the centre of the liver of a rabbit after treatment with aspartame.

Figure 8.5a: Section through the centre of the liver of a rabbit after treatment of aspartame. Note the absence of clearly distinguishable hepatocytes with no cell membranes being visible. Cords of hepatocytes were present, but appeared more like the cytoplasma of the hepatocytes formed a continuous layer. Endothelial lining of the blood vessel also not clearly distinguishable

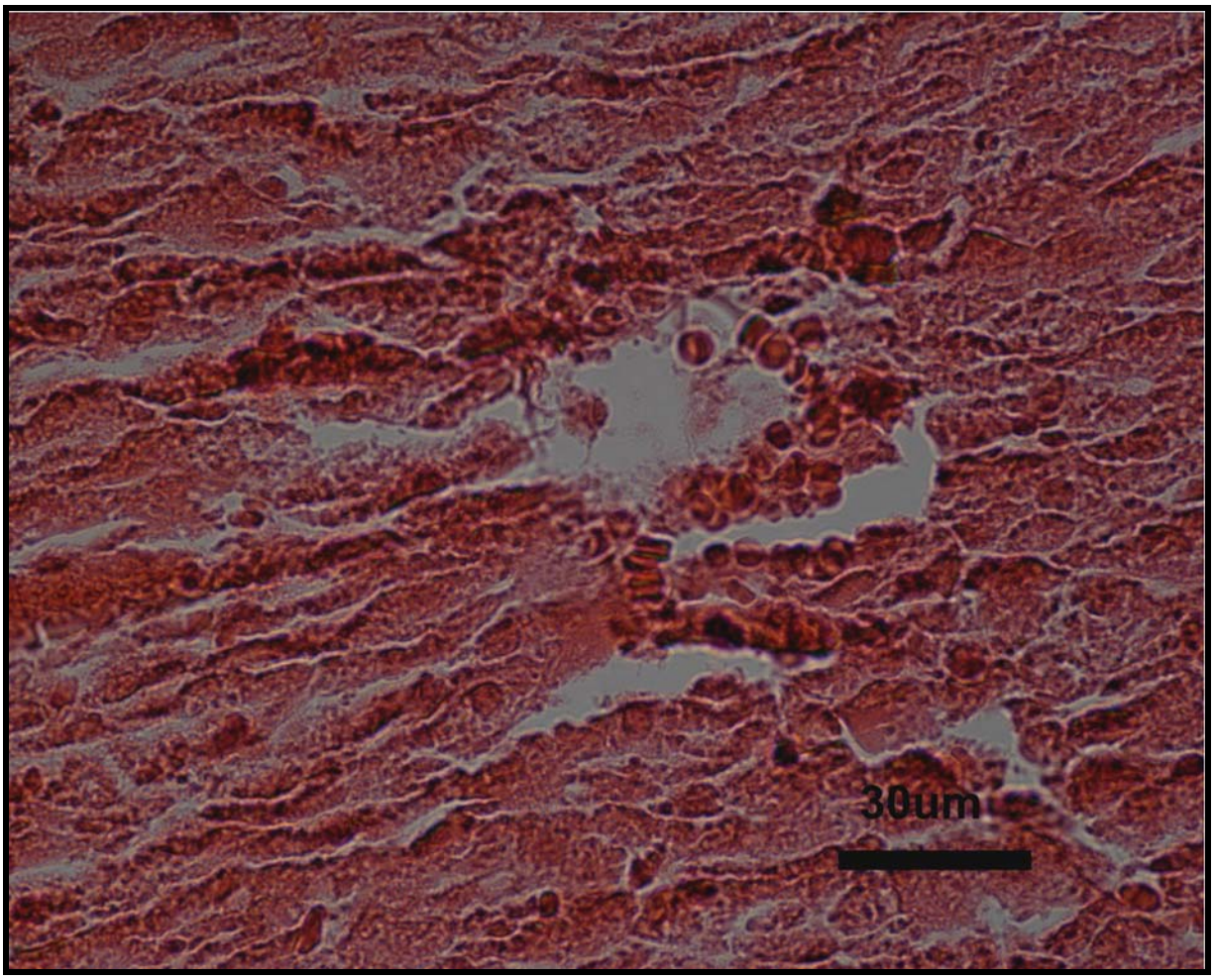

Figure 8.3b illustrates a section through the right lobe of the liver of a rabbit after treatment with aspartame.

Figure 8.3b: Section through the right lobe of the liver of a rabbit after treatment with aspartame. Cords were visible with the cellular membranes also being clear (black arrows). The cuboidal epithelium lining the duct (white arrow) was clearly distinguishable. Endothelial ling of the blood vessel appeared thinner (dashed black arrow). It appeared as though the cytoplasm of the hepatocytes were starting to become more granular, with lace-like appearance becoming more spaced and broken (circles)

Figure 8.4a and 8.4b illustrates a section through the left lobe of the liver of a rabbit treated with aspartame.

Figure 8.6a: Section through the left lobe of the liver of a rabbit after treatment with aspartame. The circles indicate hepatocytes which appear to have been damaged with the cytoplasm appearing granular, chromatin of the nuclei condensed and the cytoplasm appear to be retracting from the nuclei

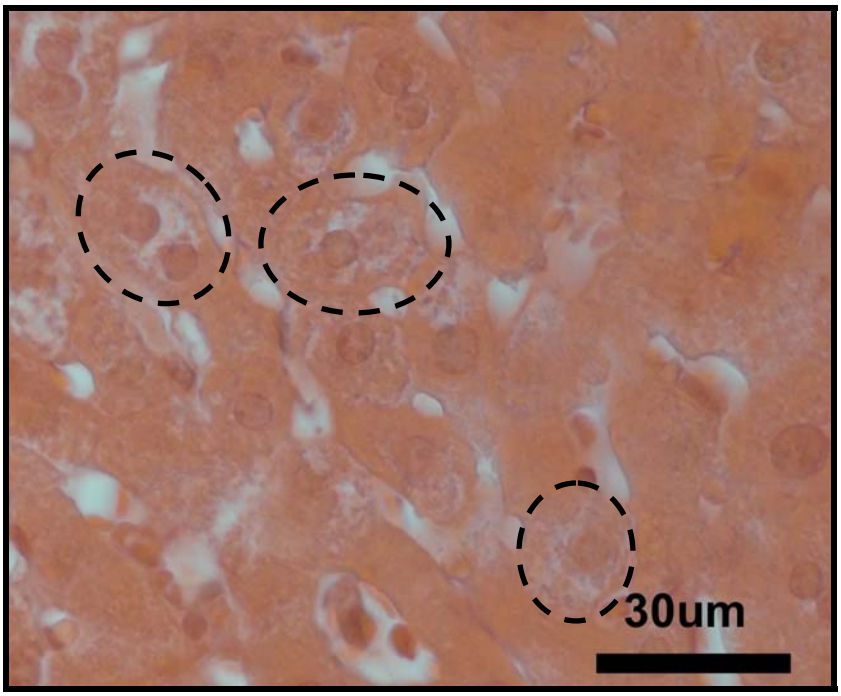

Figure 8.4b: Section through the left lobe of the liver of a rabbit after treatment with aspartame. Note the circled hepatocyte, with a clearly damaged nucleus. Chromatin appeared fragmented

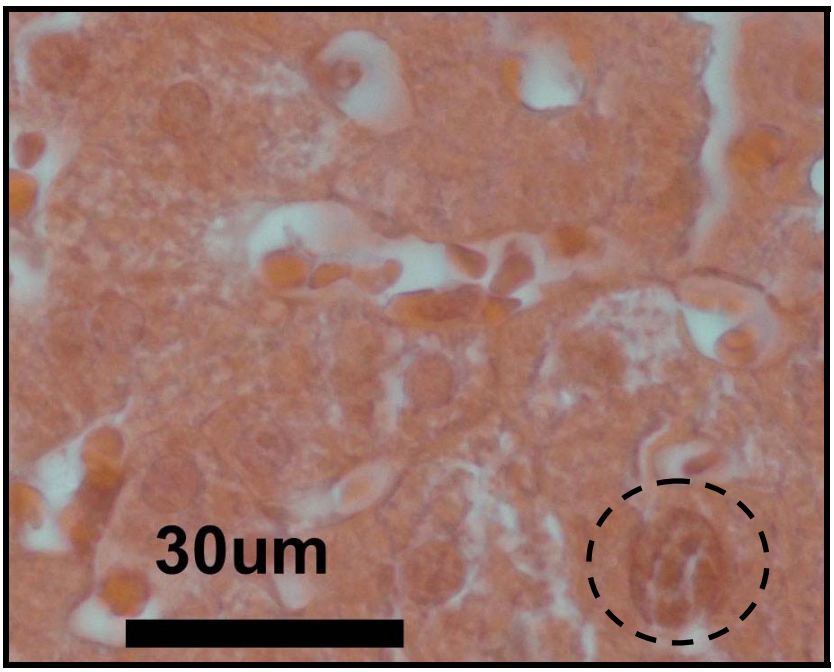

Figure 8.5 illustrates a section through the right lobe of the liver of a control rabbit.

Figure 8.5: Section through the right lobe of the liver of a control rabbit indicating a number of hepatocytes, of which three were bi-nucleate hepatocytes (circles)

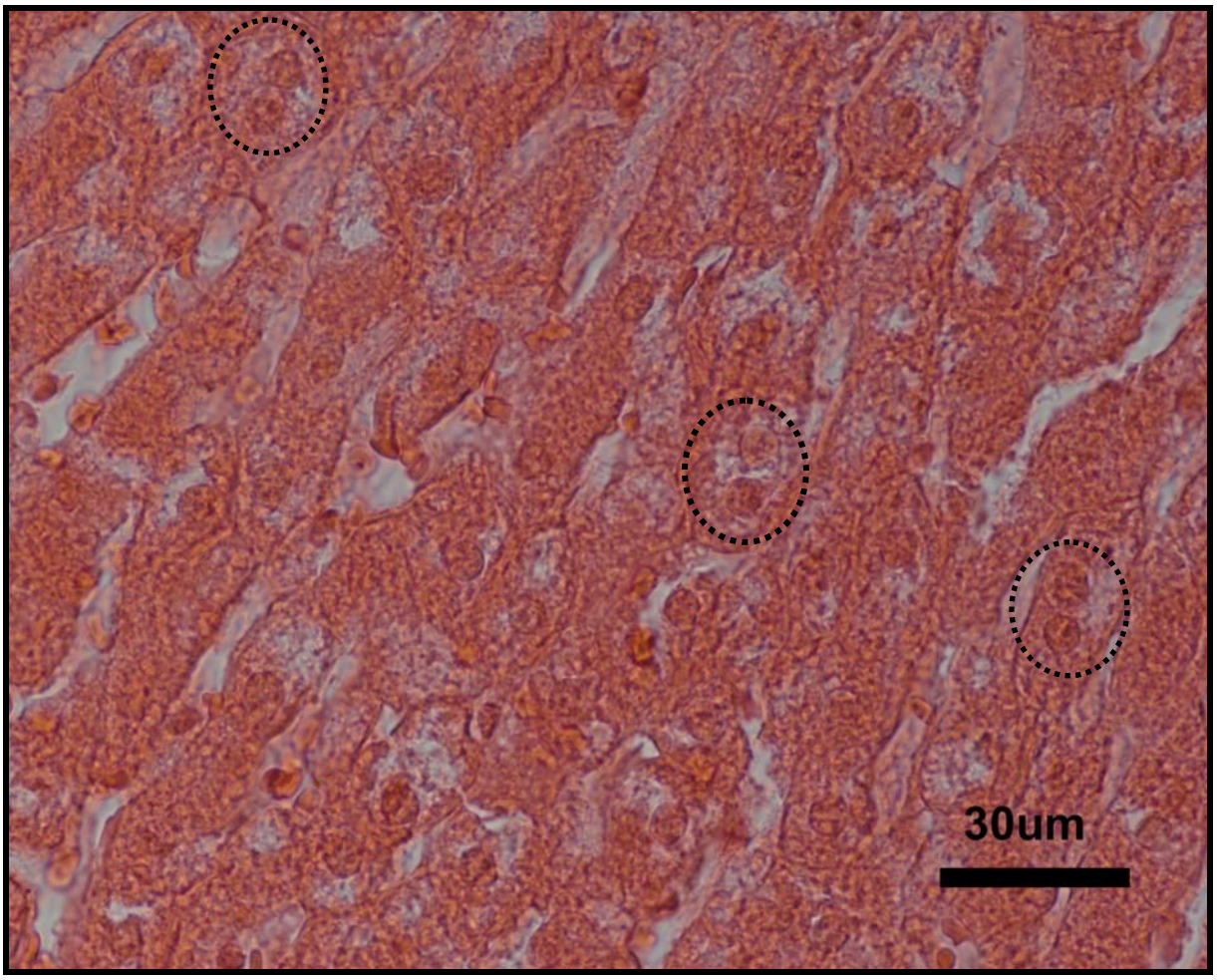

Figure 8.6 illustrates a section through the centre of the liver of a rabbit after treatment with aspartame.

Figure 8.6: Section through the centre of the liver of a rabbit after treatment with aspartame. Note the number of hepatocytes with two nuclei (circles). Cytoplasm of hepatocytes appeared more granular and chromatin inside nuclei more condensed

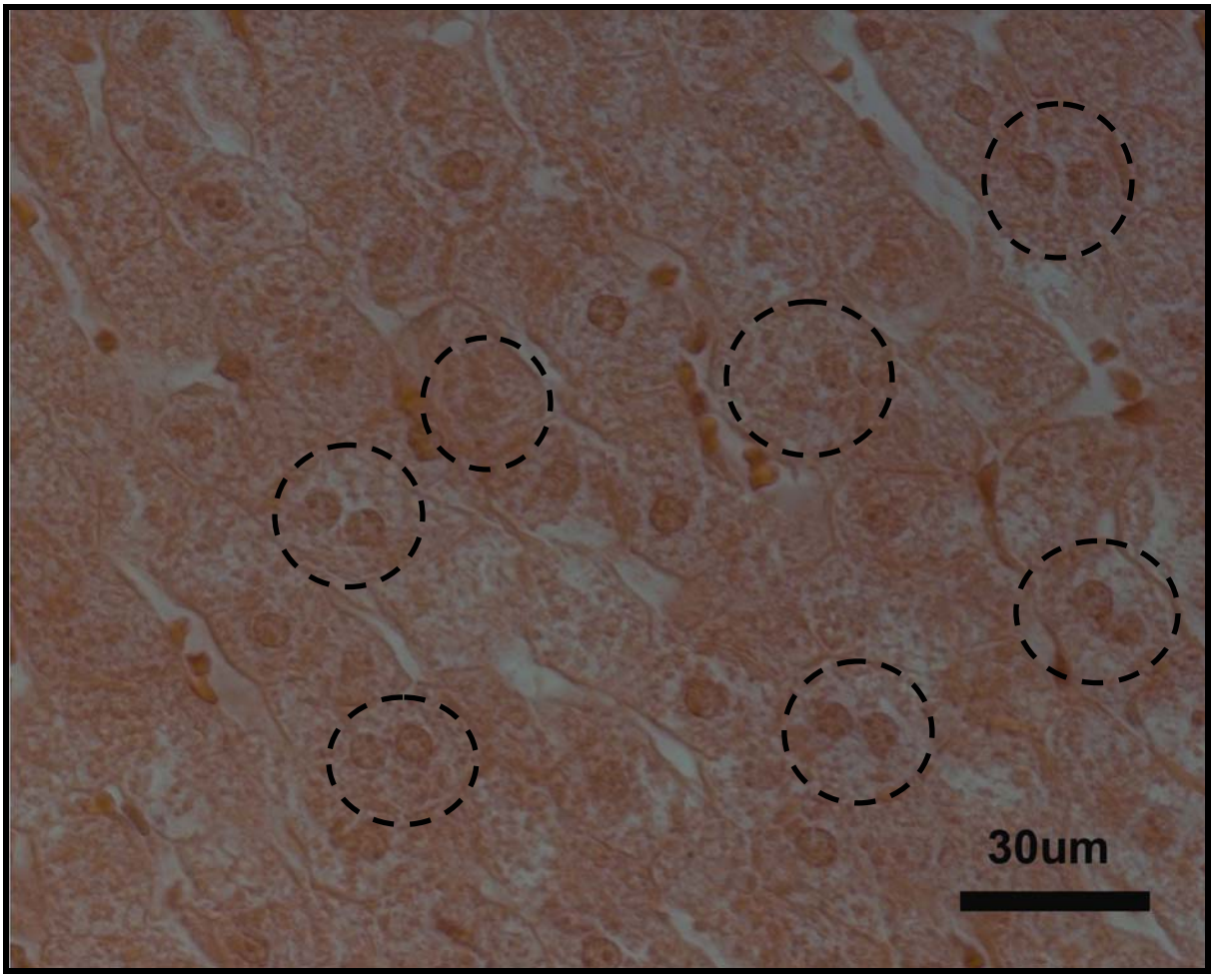

Figure 8.1a and 8.1b illustrated a section though the right lobe of the liver of a control rabbit. A central vein was visible in the centre of the illustrations containing a number of red blood cells. The endothelial lining was clearly visible (Figure 8.1b). The hepatocytes had a polygonal shape (dashed lines; Figure 8.1a) with the cellular membranes clearly visible for the different hepatocytes (Figure 8.1a and 8.1b; arrows). The nuclei of the hepatocytes had a spherical to ovoid shape with prominent, scattered chromatin granules (circle; Figure 8.1a). The cytoplasm of the hepatocytes had a lace-like appearance, possibly due to glycogen storage. Two ducts were visible in figure 8.1b, with the simple cuboidal epithelial cells having clear cellular membranes and rounded nuclei. Figure 8.2 was a section through the right lobe of the liver indicating the cords of hepatocytes that were present in the liver (dashed rectangles). Cellular membranes of the hepatocytes were clearly distinguishable, with the nuclei being prominent.

Figure 8.3a illustrated a section through the centre of the liver of a rabbit after treatment with aspartame. The cell membranes of the hepatocytes could not be identified, with the polygonal shape of the hepatocytes being absent. The nuclei of the hepatocytes were not clearly visible, with the shape ranging between round, ovoid and elongated and chromatin appeared condensed. No cords could be distinguished and it appeared as though the cytoplasm of the different hepatocytes had flown together to form one continuous layer. The endothelium of the central vein, present in the illustration could not be distinguished. Figure 8.3b was from a section through the right lobe of the liver of a rabbit after treatment with aspartame. Cords were visible with hepatocytes arranged in clear rows and cell membranes were clearly visible (arrows). The hepatocytes retained their polygonal shape, with the nucleoli being visible in the nuclei. The chromatin appeared condensed with the shape of the nuclei ranging from round to ovoid in shape (Figure 8.3b). The lace-like appearance of the cytoplasm of the hepatocytes, which had a constant pattern with a dark pink colour in the controls (Figure 8.1a), were more spaced and broken with more transparent areas being present. The cell membranes of the cuboidal epithelium lining the duct were clearly visible, with the nuclei being round (white arrow). The cytoplasm of the hepatocytes store glycogen, causing the lace-like appearance. Thus it is hypothesized that the spaces were bigger due to an increased storage of glycogen and that the pattern of the lace-like appearance could be disturbed due to damage to the hepatocytes by treatment with the aspartame. The endothelium of the central vein was clearly visible and appeared slightly thickened.

Figures 8.4a and 8.4b illustrate a section through the left lobe of the liver of a rabbit after treatment with aspartame. The hepatocytes had their characteristic polygonal shape with their nuclei appearing round to ovoid in shape. The spaced and broken appearance of the lace-like cytoplasm of the hepatocytes appeared to be more intense than the right lobe or centre of the liver, with the cytoplasm retracting/moving towards the cellular membranes. Figure 8.4b illustrates damage to the nucleus (inside circle), with the normal appearance of the scattered chromatin granules being more prominent and transparent areas starting to become visible.

The hepatocytes of the liver have a marked variation in size (polyploidy) with up to 25 percent of the cells being bi-nucleate. These bi-nuclear cells arise due to mono-nuclear cells undergoing endomitosis when nuclear volume and DNA content have approximately doubled. Mitosis is rare in adult liver cells (1 mitosis per 15 000 cells), but numerous mitotic figures can be found during repair following injury (Leeson *et al*., 1988a). More bi-nucleate cells were visible in the two aspartame treated rabbits than in the three control rabbits, after viewing under the microscope. Figure 8.5 and 8.6 represent a single eye field of a control rabbit and aspartame treated rabbit respectively. A comparison was done between the total number of cells present in both figures (Figure 8.5 and 8.6) according to nuclei that was clearly distinguishable. The following results were obtained:

Table 8.2: Comparison between the number of bi-nucleate cells in the control and aspartame treated rabbits

	Controls	Aspartame treated rabbits
Average number of cells/single eye field	35	45
Total number of single eye fields studied	15	15
Average number of bi-nucleate cells	3	7
Percentage bi-nucleate cells	8.57%	15.55%

8.57% of the hepatocytes were bi-nucleate in the control rabbit. If taken as an experimental count, this could be an indication of the normal number of bi-nucleate hepatocytes as counted in for a control in a single eye-field. It is therefore hypothesized that the increase from 8.57% to 15.55% (increase of 6.8%) could be due to mitosis to repair the damage and injury to the hepatocytes as indicated by figure 8.4a and 8.4b after treatment with aspartame.

Three sections of the liver (left lobe, right lobe and centre) were utilised for determining the effects of aspartame on the liver. For the control rabbits, there was no visible difference between the different sections of the liver. This appeared not to be the case for the rabbits treated with the aspartame. The left and right lobe showed the same level of damage, exhibiting a granular cytoplasm (lace-like appearance spaced and broken, with the cytoplasm appearing to retract from the nuclei and the chromatin becoming denser (chromatin granules more scattered) (Figures 8.3b, 8.4a and 8.4b). However, cell membranes and cords of hepatocytes were still visible. The effect of the aspartame on the centre of the liver was far more pronounced as the effect on the left and the right lobes. The cell membranes of the hepatocytes could not be distinguished with the cytoplasm of the different hepatocytes appearing as one continuous layer. The cords of the hepatocytes could not be distinguished (Figure 8.3a). Figure 8.5 illustrated the centre of the liver with seven different hepatocytes

having bi-nucleate nuclei. If the hypothesis that there was an increase in the number of bi-nucleate hepatocytes between the control and aspartame treated rabbits was accepted, three of the seven bi-nucleate hepatocytes (8.57% of 45 hepatocytes subtracted from seven hepatocytes with bi-nucleate nuclei) was busy undergoing mitosis to repair the damage and injury brought about by the treatment with aspartame. These result lead to the hypothesis, that the larger the distance from the centre of the liver, the less outspoken the effect of aspartame on the hepatocytes, but an effect will be present and due to the damage to the hepatocytes that the liver attempts to replace the damaged hepatocytes. Results obtained in chapter 5 of this thesis, support the microscopic findings that the liver must have been damaged as three of the five factors (F VII, F X and fibrinogen) produced and secreted by the liver were affected after treatment with aspartame. In humans, if both F VII and F X concentrations are decreased, prolonged hepatitis is diagnosed (Package insert – STA Deficient X; Ref 00738), thus it is hypothesized that this could also have been a possibility in this study. Phenylalanine is converted to tyrosine in the liver by phenylalanine hydroxylase. Thus it is hypothesized that due to the damage to the hepatocytes, the liver could be unable to convert aspartame to tyrosine, thus the level of phenylalanine in the blood was high, thus increasingly suppressing tryptohan conversion to serotonin as tryptophan cannot be carried over the BBB.

8.3.2 Microscopic study of the histological morphology of the kidney

8.3.2.1 Cortex of the kidney

Figure 8.7a and 8.7b illustrates renal corpuscles and the medullary rays of the kidney of a control rabbit.

Figure 8.7a: Cortex of the kidney of a control rabbit illustrating a number of renal corpuscles (circles) and tubules

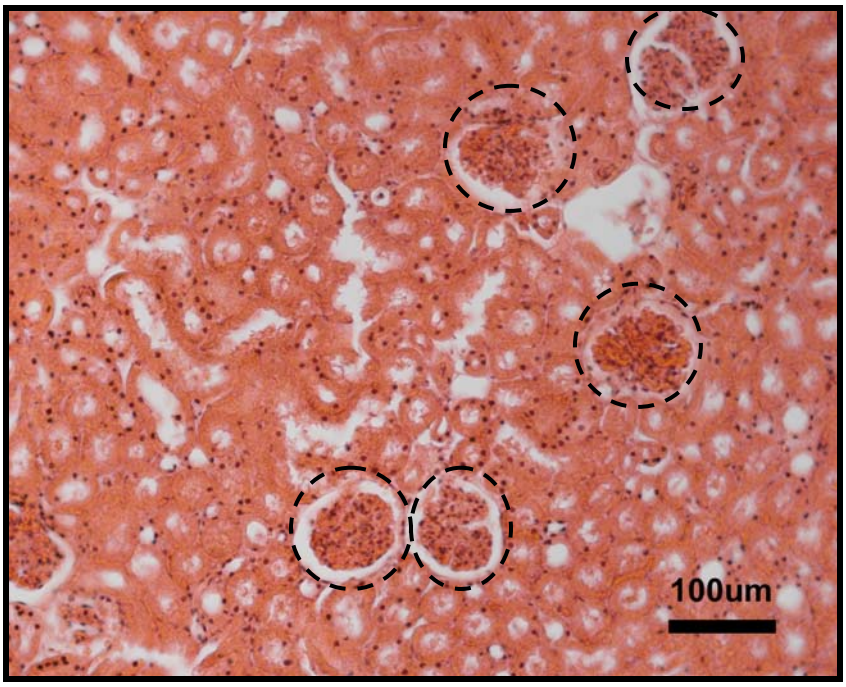

Figure 8.7b: Cortex of the kidney of a control rabbit illustrating renal corpuscles (circles) and the medullary rays (arrows) present in the cortex

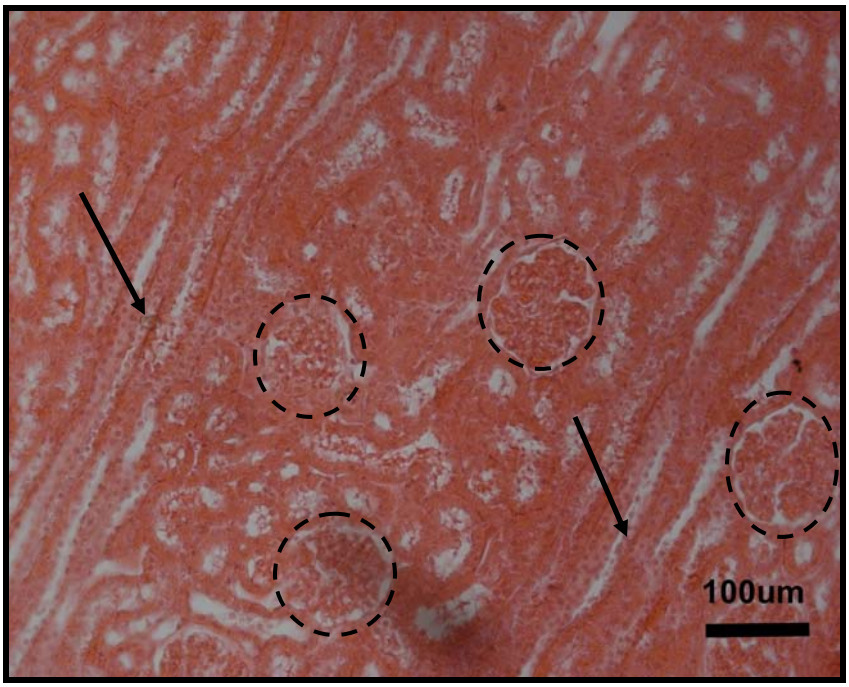

Figure 8.8 illustrates the renal corpuscle of a control rabbit at a higher magnification.

Figure 8.8: Renal corpuscle of a control rabbit. Label A – extraglomerular mesangial cells; Label B – vascular pole; Label C – glomerulus; Label D – mesangial cells; Label E – urinary space; Label F – parietal layer of Bowman's capsule; Label G - Nucleus of podocyte

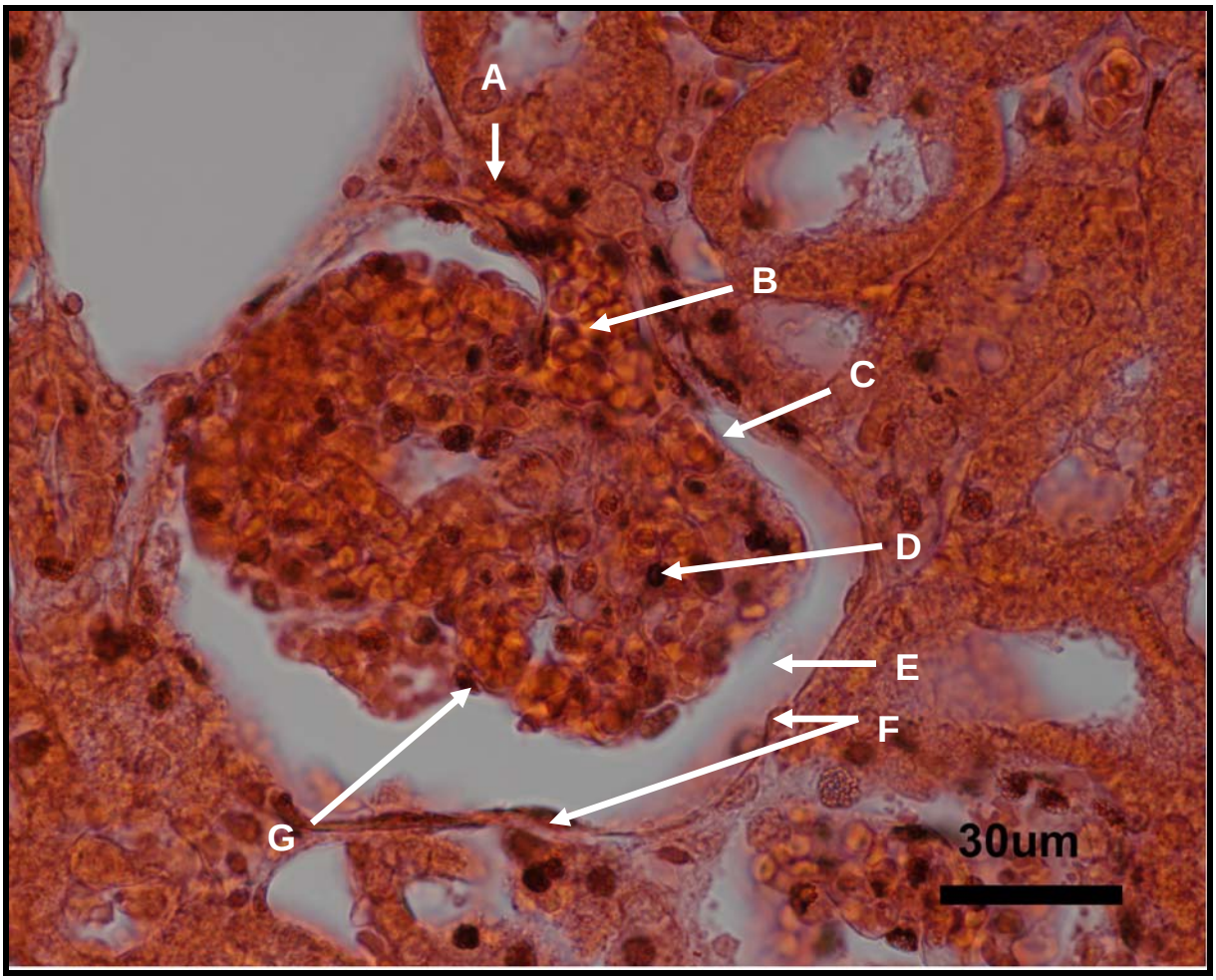

Figure 8.9a and 8.9b illustrates the layers of Bowman's capsule of a control rabbit at a higher magnification.

Figure 8.9a: Parietal layer of the capsule of Bowman in a control rabbit (arrows)

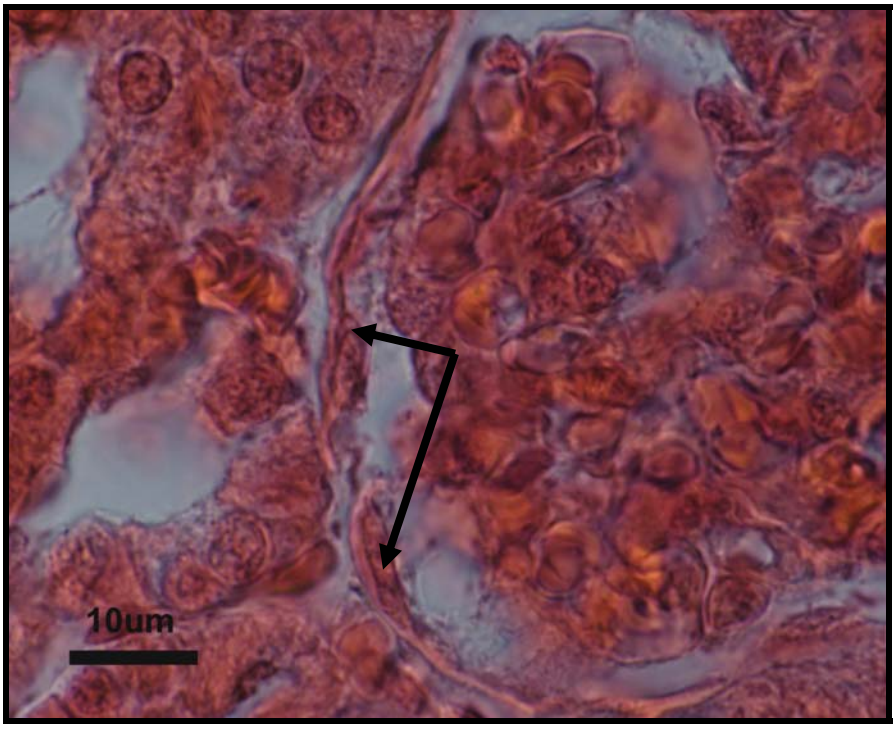

Figure 8.9b: Visceral layer of the capsule of Bowman in the control rabbit (arrows). The dashed arrow indicates the nucleus of a podocyte

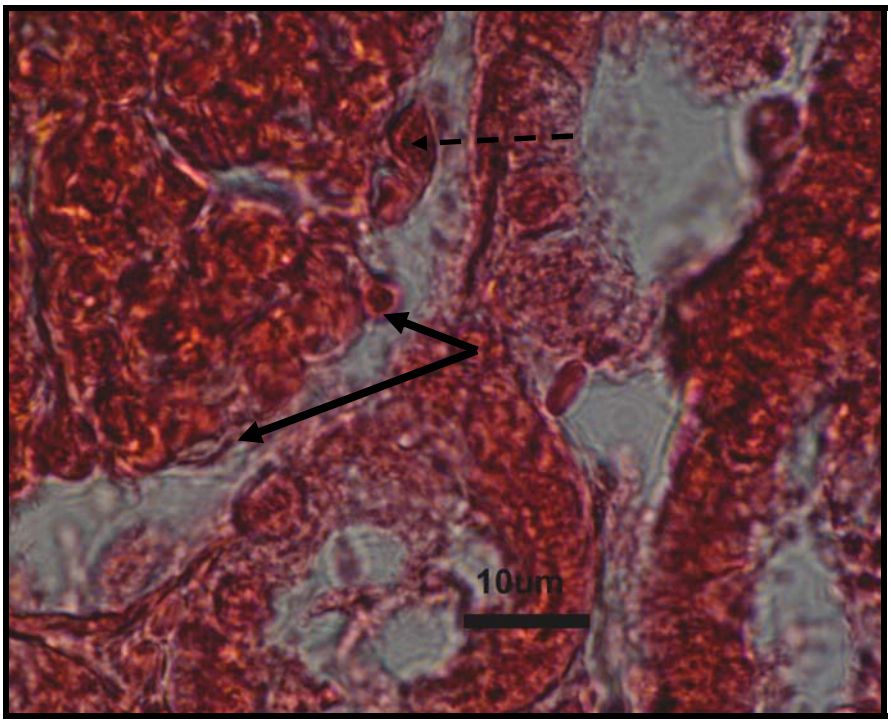

Figure 8.10 illustrates the renal corpuscles and medullary rays of a rabbit after treatment with aspartame.

Figure 8.10: Cortex of the rabbit treated with aspartame, illustrating the renal corpuscles (circles) and the medullary rays (arrows). The dashed arrow indicates damage to cellular membranes of cuboidal epithelium lining the tubules

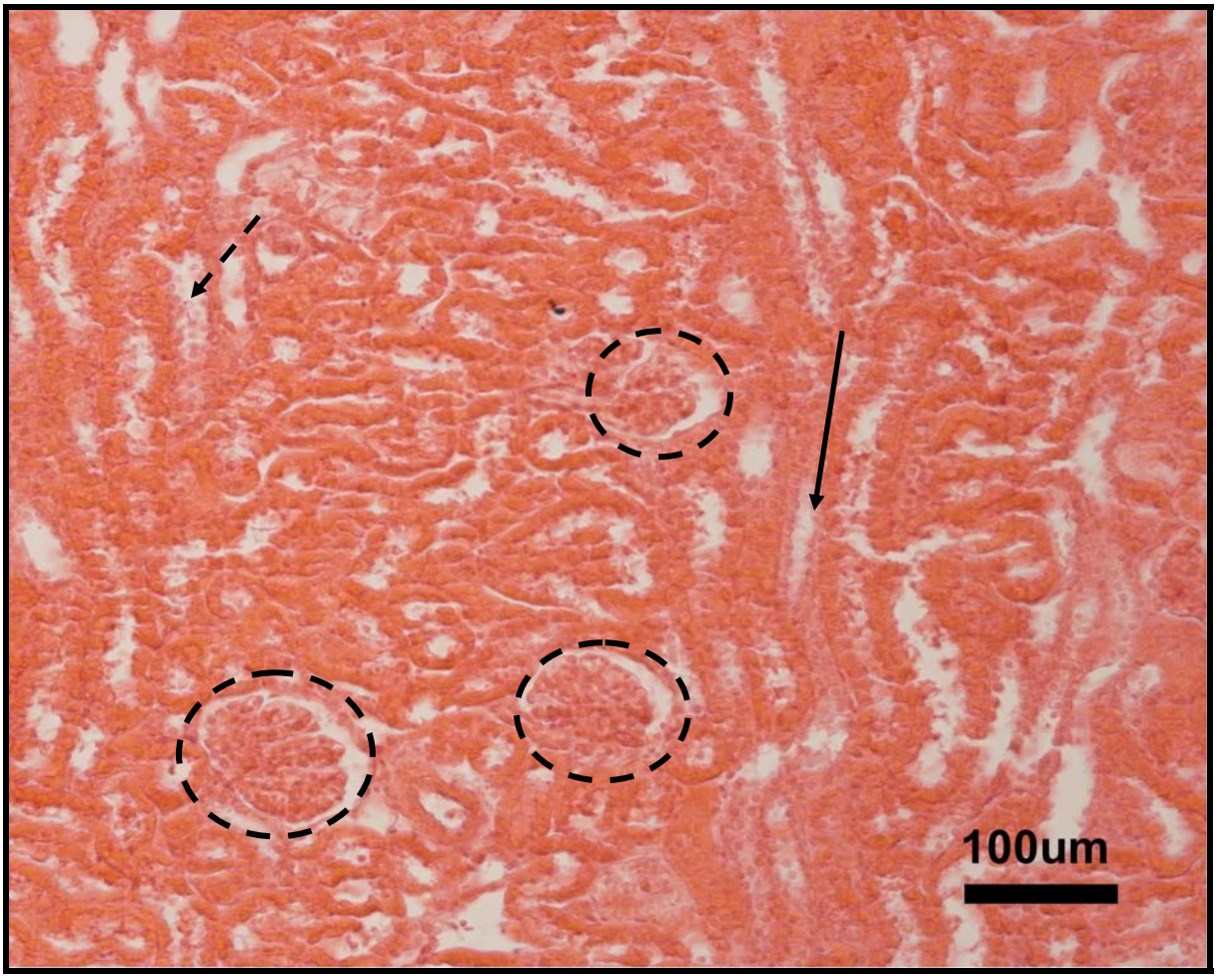

Figure 8.11 illustrates the renal corpuscle of an aspartame treated rabbit.

Figure 8.11: Glomerulus of an aspartame treated rabbit. Label A – extraglomerular mesangial cells; Label B – vascular pole; Label C – glomerulus with mesangial cells; Label D – urinary space; Label E – parietal layer of Bowman's capsule; Label F – nucleus of podocyte

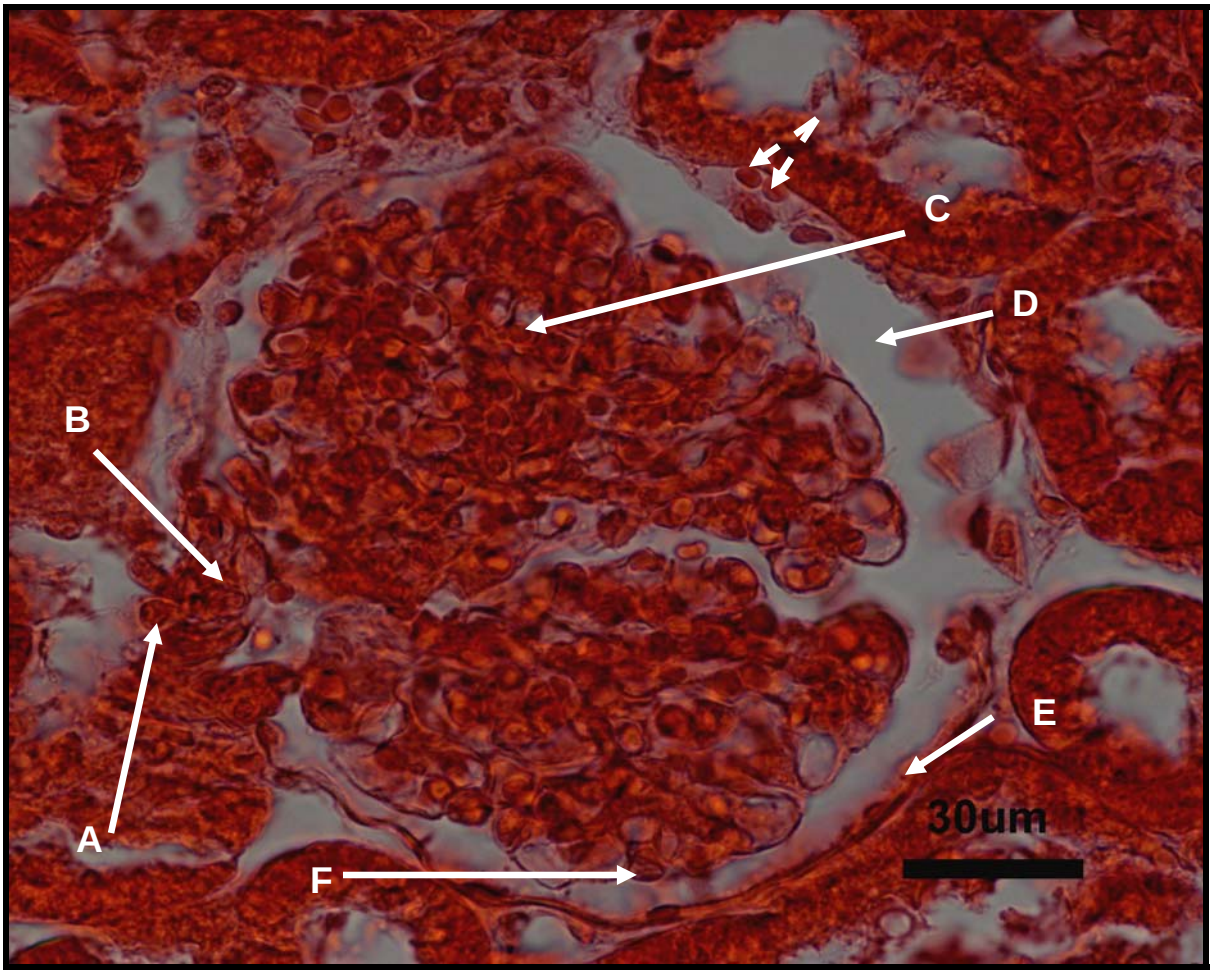

Figure 8.12a and 8.12b illustrates the layer of Bowman's capsule at a higher magnification.

Figure 8.12a: Parietal layer of the capsule of Bowman of a rabbit after treatment with aspartame (arrows)

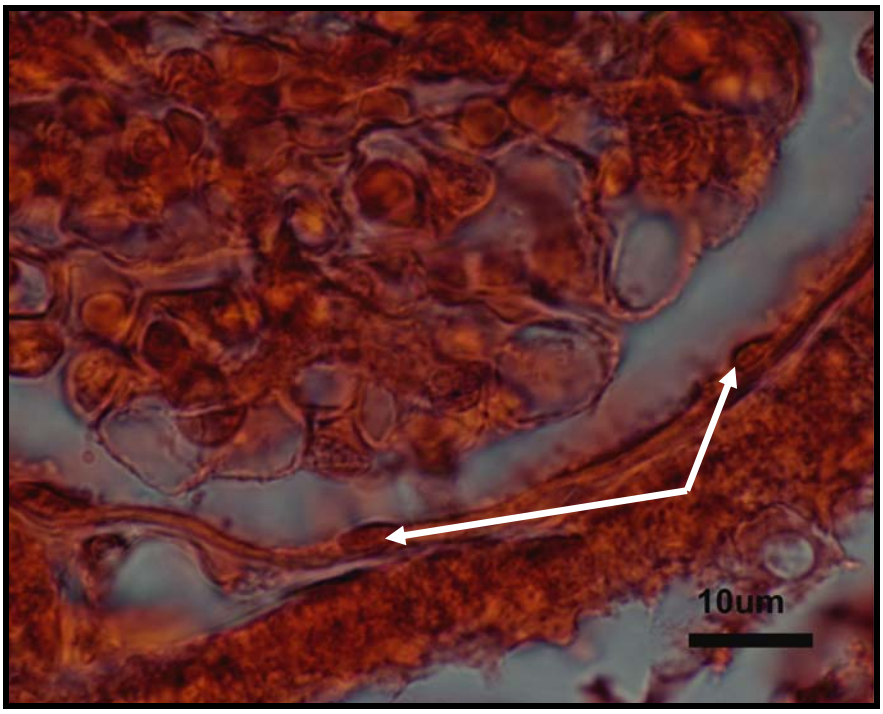

Figure 8.12b: Visceral layer of the capsule of Bowman of a rabbit after treatment with aspartame (arrows)

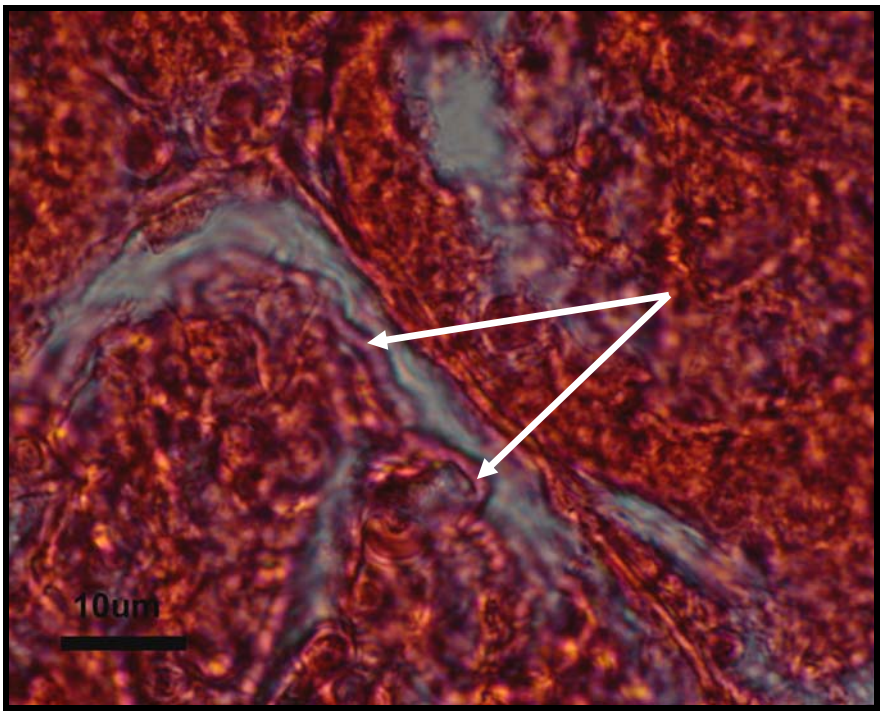

Figure 8.7a and 8.7b illustrated the renal corpuscles and medullary rays that were present in the cortex of a control rabbit. The urinary space surrounding the glomeruli of the renal corpuscles was clearly visible, even at low magnification. Figure 8.8 illustrated a renal corpuscle of a control rabbit at a higher magnification. The extra-glomerular mesangial cells (Label A) were visible at the vascular pole (Label B) of the renal corpuscle and the urinary space (Label D) could also be distinguished. The parietal layer of the capsule of Bowman (Label E) was noted with the simple squamous epithelium having clear flat nuclei which very slightly protruded into the urinary space. A nucleus of a podocyte (Label F) of the visceral layer of the capsule of Bowman was visible. Figure 8.9a and 8.9b illustrated the different layers of the capsule of Bowman, only at a higher magnification. The simple squamous epithelium with the flattened nuclei could be distinguished (arrow; Figure 8.9a). The visceral layer, consisting of podocytes (dashed arrow; Figure 8.9b) was visible as a very thin line on the outer surface of the glomerulus.

Figure 8.10 illustrated the cortex of a rabbit after treatment with aspartame. The renal corpuscles were clearly visible, with the urinary space (circles) appearing enlarged. The tubules found in the medullary rays (arrow) appeared damaged (dashed arrow) as the cellular membranes could not be distinguished. It appeared as though the nuclei of the simple cuboidal epithelium lining the tubules were spilling into the lumen of the tubules.

Figure 8.11 illustrates a renal corpuscle at a higher magnification. Extra-glomerular mesangial cells were visible (Label A) at the vascular pole (Label B) of the renal corpuscle. A number of mesangial cells were visible between the capillaries of the glomerulus (Label C), which appeared to have increased (more nuclei visible than in control) and both layers of Bowman's capsule were very clear. Erythrocytes were visible underneath the parietal layer of Bowman's capsule (dashed arrows; Label E) and the layer itself appeared thickened. The visceral layer of the capsule of Bowman (Label F) investing the capillaries of the glomerulus were clearly visible (Label G). When these layers were studied at a higher magnification (Figures 8.12a and 8.12b), both the parietal and visceral layers appeared to have thickened. The visceral layer that was not visible at first glance for the control rabbit (Figure 8.9b), was very clearly distinguishable after treatment with aspartame (Figure 8.12b).

8.3.2.2 Medulla of the kidney

Figure 8.13 illustrates the medulla with the collecting tubules in a control rabbit.

Figure 8.13: Collecting tubules in the medulla of a control rabbit. Arrows indicate the cuboidal epithelium of the proximal convoluted tubules. Note the clearly distinguishable cellular membranes

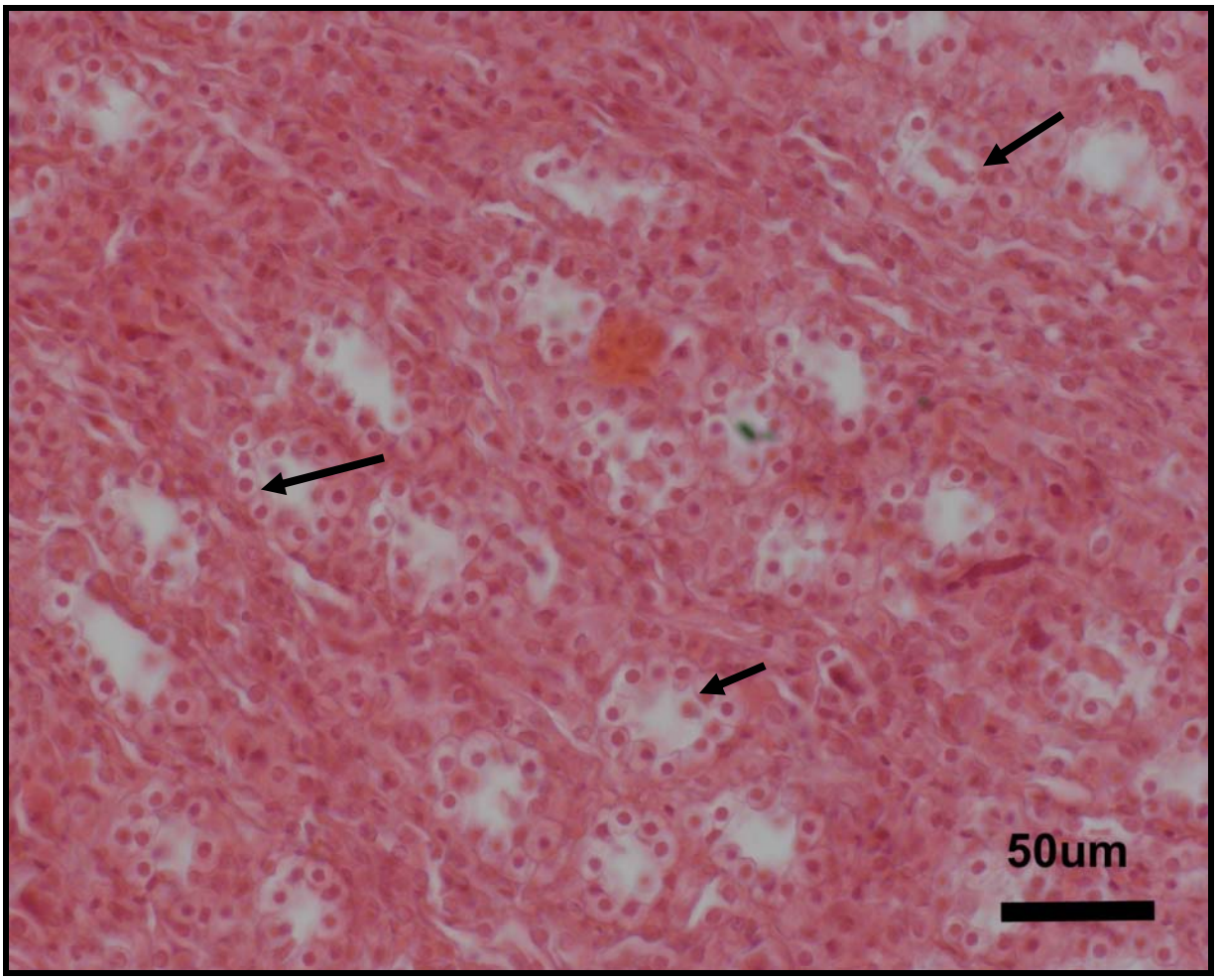

Figure 8.14 indicates the squamous epithelium of thin segment of the Loop of Henle's in a control rabbit.

Figure 8.14: Squamous epithelium of the thin segment of the loop of Henle's in the control rabbit (arrows)

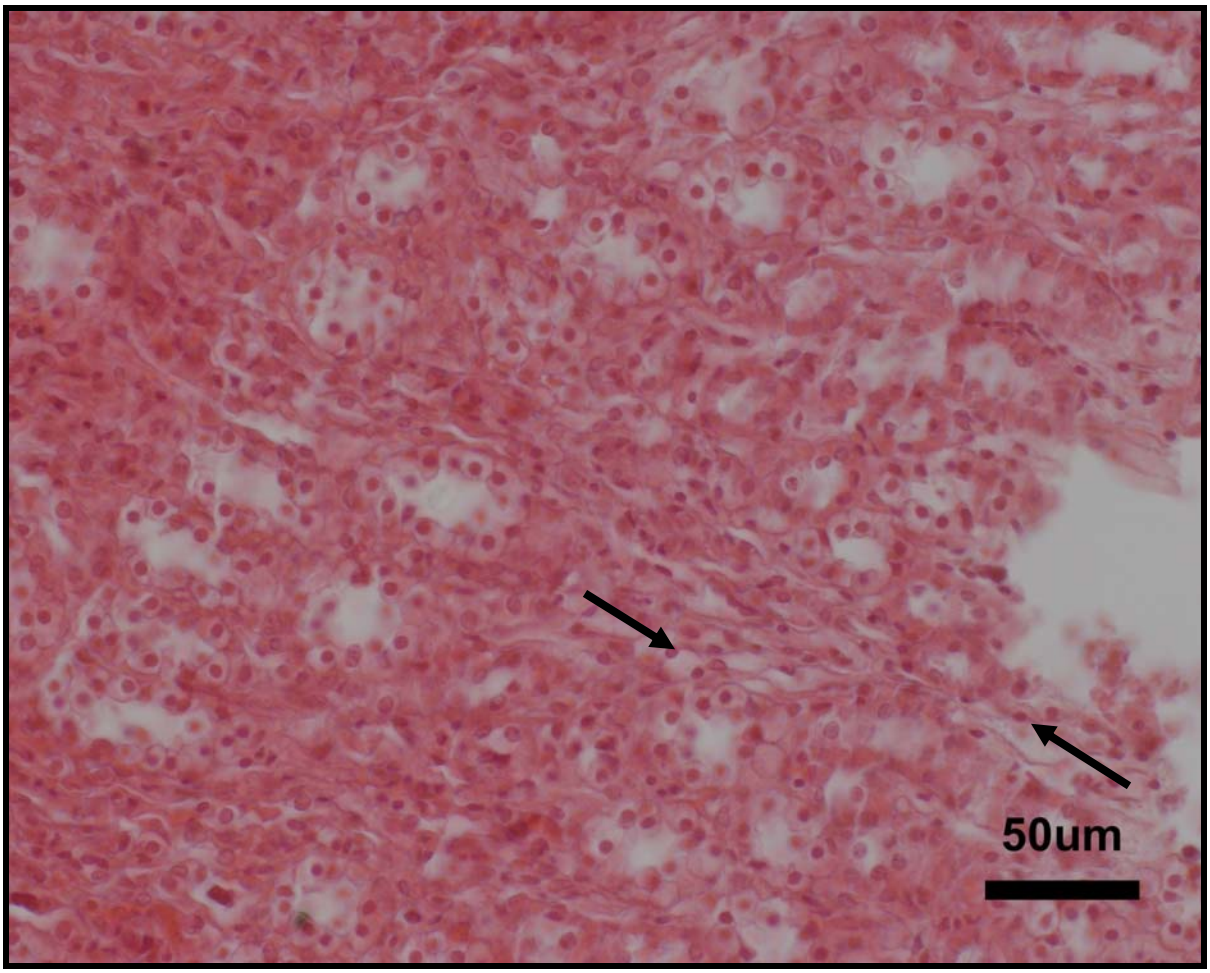

Figure 8.15a and 8.15b illustrates the cuboidal and squamous epithelium of the proximal convoluted tubule and thin segment of the loop of Henle's respectively in a control rabbit at higher magnifications (x40 and x 100 respectively). Figure 8.15c illustrates an endothelial cell of a control rabbit.

Figure 8.17a: Arrow indicates the cuboidal epithelium of the proximal convoluted tubule and the dashed arrow indicate the squamous epithelium of the thin segment of the loop of Henle's in a control rabbit

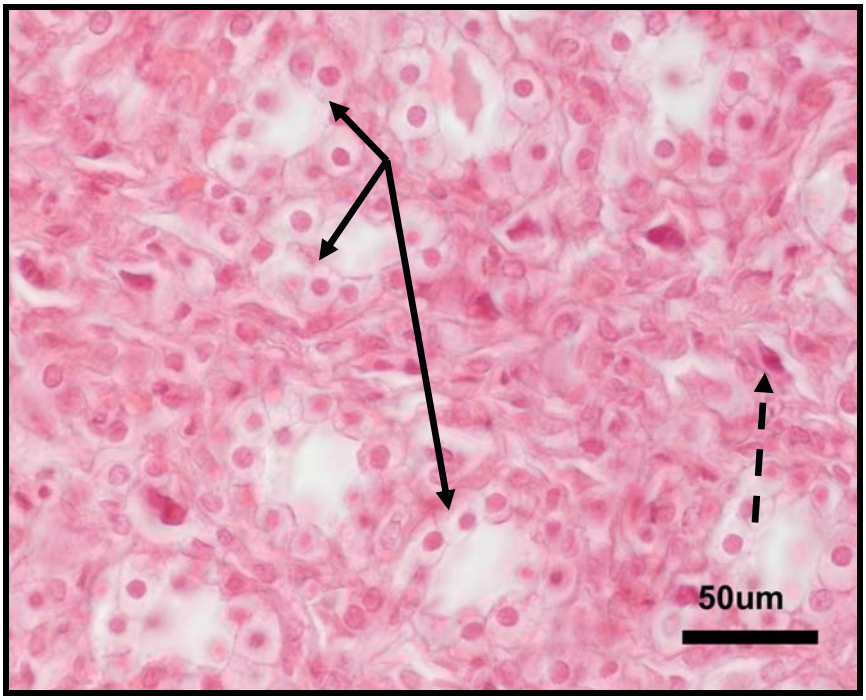

Figure 8.15b: Arrow indicates the cuboidal epithelium of the proximal convoluted tubule in a control rabbit. Note the clearly distinguishable cellular membranes. The dashed arrow indicates the squamous epithelium of the thin segment of the loop of Henle's

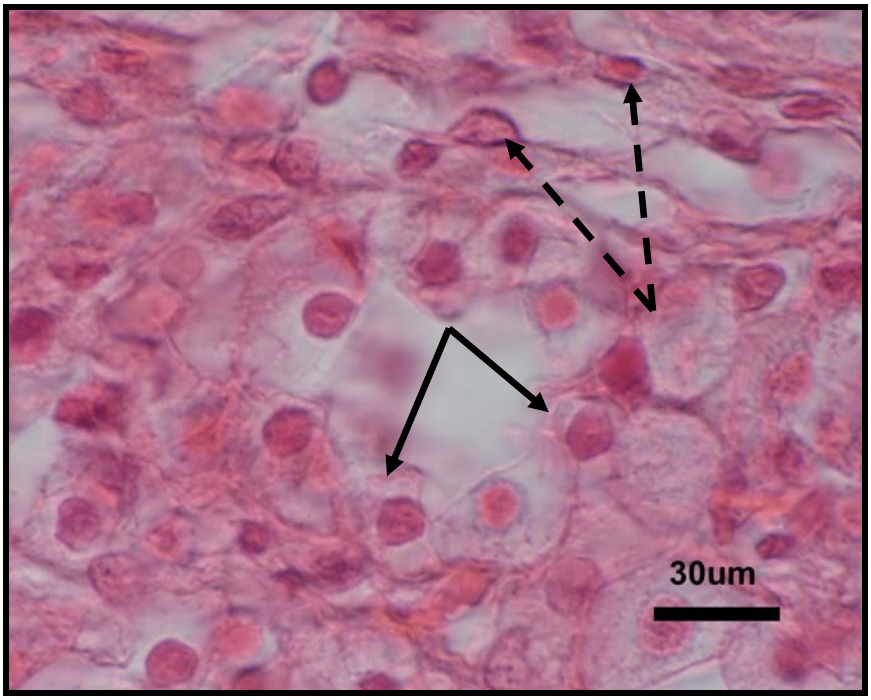

Figure 8.15c: Endothelial cell (arrow) inside the vasa recta of a control rabbit. Note the flattened, ovoid shape of the nucleus

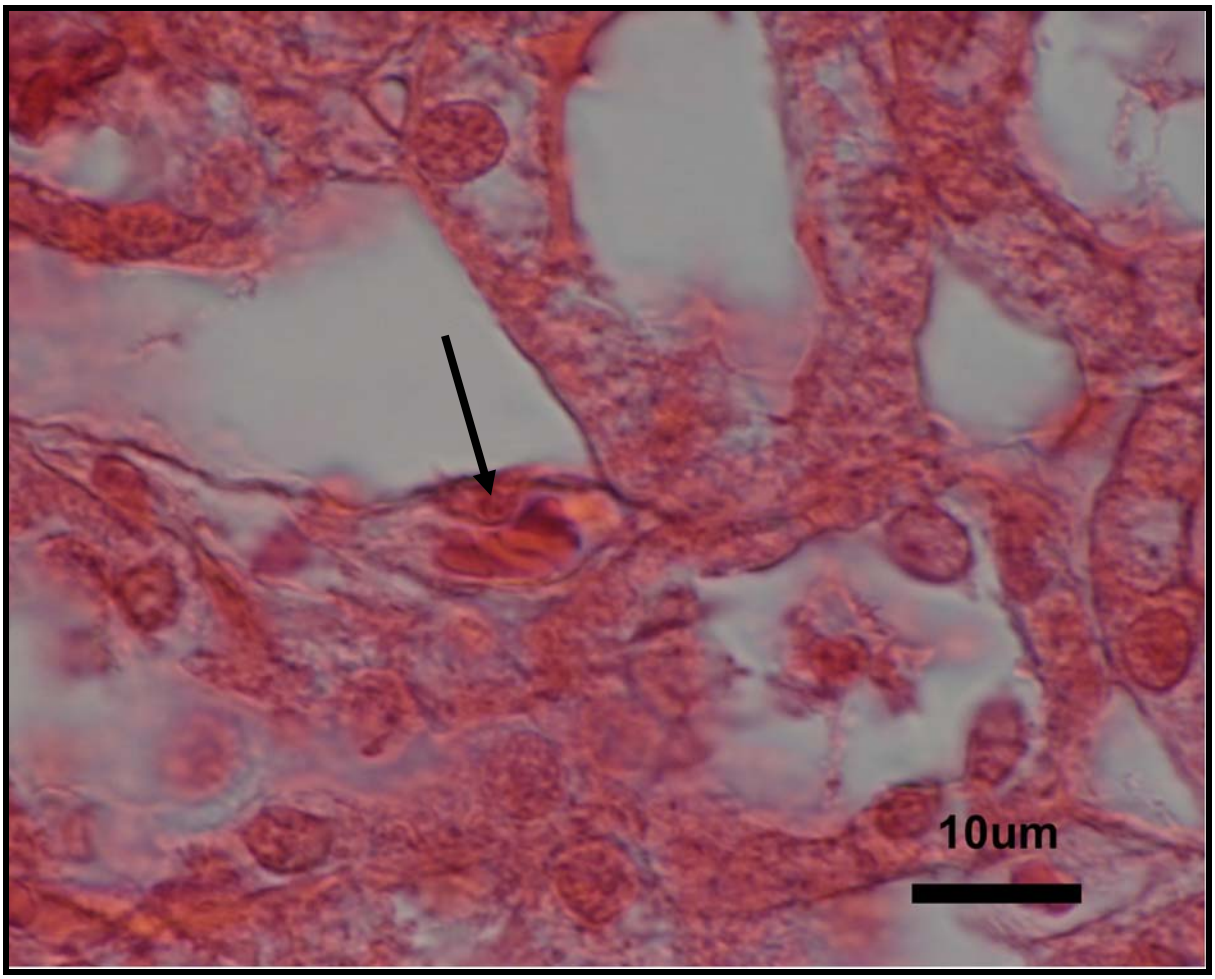

Figure 8.16 illustrates the medulla with the collecting tubules in an aspartame treated rabbit.

Figure 8.16: Collecting tubules in the medulla of an aspartame treated rabbit. Arrows indicate the cuboidal epithelium of the proximal convoluted tubules. Note that the cellular membranes have suffered damage

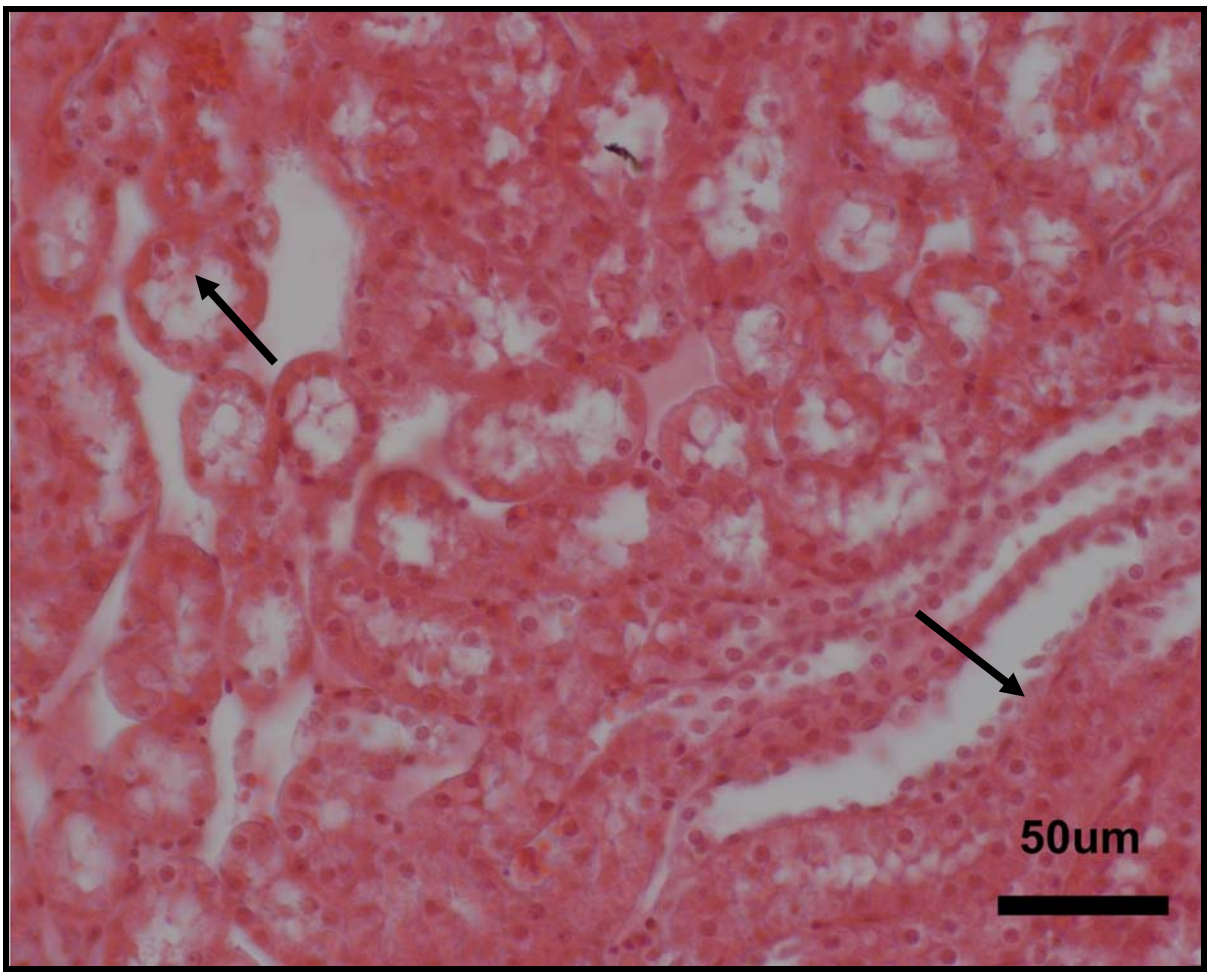

Figure 8.17 indicates the squamous epithelium of thin segment of the Loop of Henle's in a aspartame treated rabbit.

Figure 8.17: Squamous epithelium of the thin segment of the loop of Henle's in the aspartame treated rabbit (arrows). Note the rounded nucleus of an endothelial cell (dashed arrow) inside the vasa recta

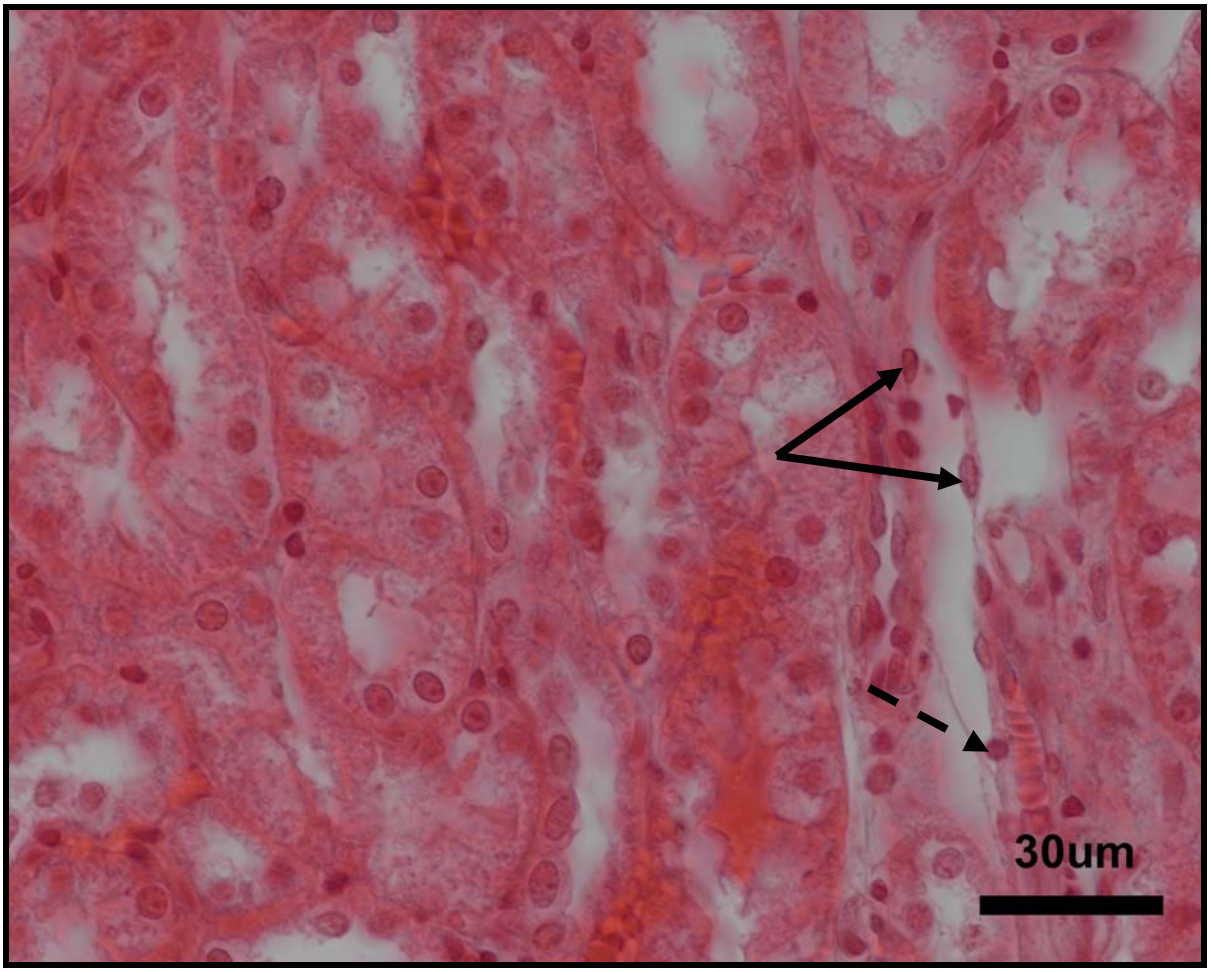

Figure 8.18a illustrates the cuboidal and squamous epithelium of the proximal convoluted tubule and thin segment of the loop of Henle's respectively and figure 8.18b illustrates the endothelium lining in an aspartame treated rabbit at higher magnifications (x40 and x 100 respectively).

Figure 8.18a: Cuboidal epithelium of the proximal convoluted tubule (arrows) and squamous epithelium of the thin segment of the loop of Henle's (dashed arrows) in the aspartame treated rabbits. The cytoplasm of the cuboidal cells appeared washed-out. Damaged cellular membranes of the cuboidal epithelium were also present (white arrows)

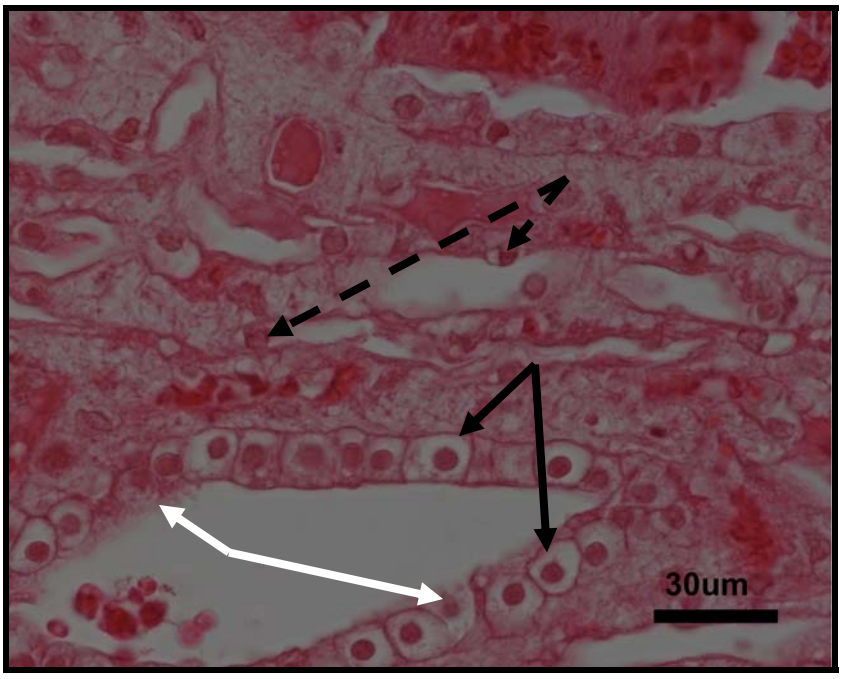

Figure 8.18b: Endothelial lining of the vasa recta in an aspartame treated rabbit. Note the rounded, not flat, nucleus of the endothelial cell (arrow)

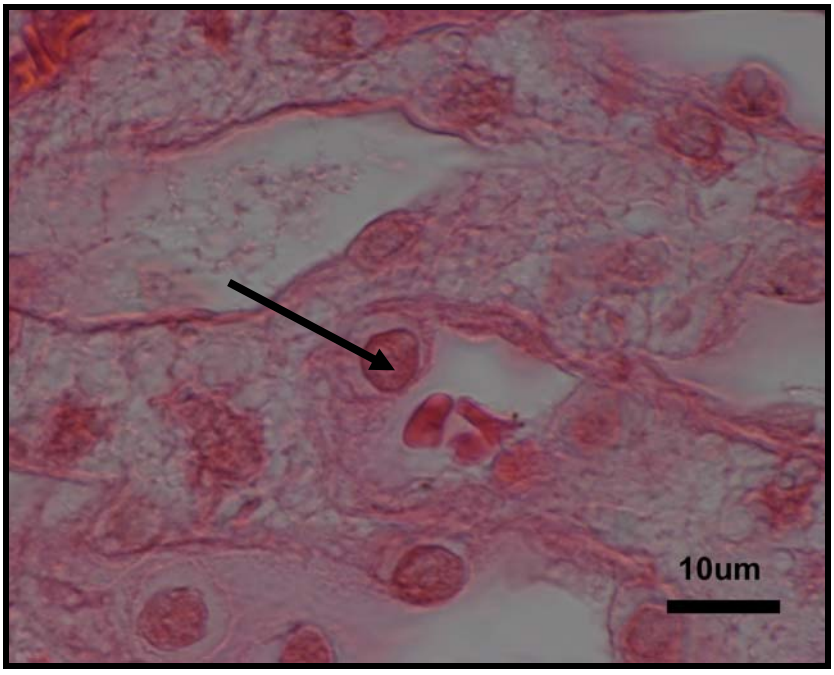

Figure 8.13 illustrated the collecting tubules in the medulla of a rabbit after treatment with aspartame. The cuboidal epithelium lining the proximal convoluted tubule (arrows) could be distinguished, with clearly visible cellular membranes. Figure 8.14 illustrated the simple squamous epithelium lining (arrows) the thin segment of the loop of Henle's in the medulla of the kidney of a control rabbit. The cellular membranes were clearly visible and their flattened nuclei could be easily distinguished. Figure 8.15a and 8.15b illustrated the cuboidal (arrows) and squamous epitheliums (dashed arrows) of the proximal convoluted tubule and thin segment of the loop of Henle's respectively at a higher magnification. Cellular membranes were clearly visible for both epitheliums. The cytoplasm of the cuboidal epithelium stained light pink with filament-like structures being visible. The nuclei of the squamous epithelium had their characteristic flattened, elongated shape. Figure 8.15c illustrated the nucleus of an endothelial cell of the vasa recta, with its characteristic flattened ovoid shape.

Figure 8.16 illustrated the collecting tubules in the medulla of the kidney of a rabbit after treatment with aspartame. The cuboidal epithelium lining the proximal convoluted tubule appeared damaged as no clear cellular membranes could be distinguished (arrows). Figure 8.17 illustrated the squamous epithelium that lines the thin segment of the loop of Henle's, with the nuclei appearing more rounded in shape (arrows). The nucleus of an endothelial cell of the vasa recta was also visible (dashed arrow), but it did not have its characteristic flattened shape, it was round. At a higher magnification, the cytoplasm of the cuboidal epithelium appeared transparent (Figure 8.18a) and the filament-like structures that were present in the controls (Figure 8.15b) were very few to absent in the rabbits after treatment with aspartame. The nuclei of the squamous epithelium appeared rounder (Figure 8.18b) as when compared to those in the controls (Figure 8.15b). Figure 8.18b illustrated the nucleus of an endothelial cell of the vasa recta in a rabbit after treatment with aspartame. The nucleus had lost its characteristic flatted shape and became round.

8.4 SUMMARY AND EXPLANATION

Table 8.3 summarizes the differences found in the livers of the control and aspartame treated rabbits.

Table 8.3: Comparative summary between the control and aspartame treated rabbits after treatment with aspartame with special attention to the sections of the liver from which it was obtained

	Control	Aspartame – Centre of liver	Aspartame – Right lobe liver	Aspartame – Left lobe liver
Endothelium of central vein	Clearly visible (Right lobe liver; Fig. 8.1b)	Could not be distinguished (Fig. 8.3a)	Clearly visible; appeared thickened (Fig. 8.3b)	No vein present
Shape of hepatocyte	Polygonal shape (Right lobe liver; Fig. 8.1a)	Could not be distinguished (Fig. 8.3a)	Polygonal shape (Fig. 8.3b)	Polygonal shape (Fig. 8.4a)
Shape of nuclei of hepatocytes	Spherical to ovoid in shape	Not clearly visible; nuclei had round, ovoid elongated shape (Fig. 8.3a)	Round to ovoid in shape with nucleoli visible (Fig. 8.3b)	Round to ovoid (Fig. 8.4a)
Chromatin of nuclei of hepatocytes	Prominent scattered chromatin granules (Right lobe liver; Fig. 8.1a)	Condensed (Fig.8.3a)	Condensed (Fig. 8.3b)	Damage to nuclei – scattered pattern of chromatin granules more prominent with transparent areas becoming visible (Fig. 8.4b)
Cellular membranes of hepatocytes	Clearly visible (Right lobe liver; Fig.8.1a and 8.1b)	Could not be distinguished (Fig. 8.3a)	Clearly visible (Fig. 8.3b)	Clearly visible (Fig. 8.4a)
Cytoplasm of hepatocytes	Lace-like appearance (Right lobe liver; Fig. 8.1a)	Flown together (Fig. 8.3a)	Lace-like appearance more spaced and broken; transparent areas present (Fig. 8.3b)	Spaced and broken appearance more intense; retracting towards cellular membranes (Fig. 8.4a)

Table 8.3 (continue): Comparative summary between the control and aspartame treated rabbits after treatment with aspartame with special attention to the sections of the liver from which it was obtained

	Control	Aspartame – Centre of liver	Aspartame – Right lobe liver	Aspartame – Left lobe liver
Simple cuboidal epithelium of ducts	Clear cellular membranes with rounded nuclei (Right lobe liver; Fig. 8.2)	No ducts present	Clearly visible with round nuclei (Fig. 8.3b)	Not present
Cords of the hepatocytes	Cellular membranes clearly distinguishable; nuclei prominent (Right lobe liver; Fig. 8.2)	No cords could be distinguished (Fig. 8.3a)	Visible; Hepatocytes in clear rows	Not present

Table 8.4 illustrates a comparative summary of the cortex of the kidney of the control and aspartame treated rabbits to illustrate the possible effects of aspartame.

Table 8.4: Comparative summary of the cortex of the kidney of both the control and aspartame treated rabbits to illustrate the possible effects of aspartame

	Control rabbits	**Aspartame treated rabbits**
Urinary space	Clearly visible (Fig. 8.7a and 8.7b)	Appears enlarged
Extra-glomerular mesangial cells	Clearly visible at vascular pole (Fig. 8.8; Label A and B)	Visible at vascular pole (Fig. 8.11; Label A and B)
Mesangial cells	Visible (Fig. 8.8; Label D)	Visible; appeared to have an increase in the number of cells (more nuclei visible) (Fig. 8.11; Label C)
Parietal layer of the capsule of Bowman	Simple squamous epithelium with flattened nuclei (Fig. 8.8; Label E) (Fig. 8.9a)	Erythrocytes captured below parietal layer (dashed arrows; Fig. 11; Label E); appeared thickened (Fig. 8.12a)
Visceral layer of the capsule of Bowman	Nucleus of podocyte visible Fig. 8.8; Label F). Layer very thin (Fig. 8.9b)	Clearly visible (Fig. 8.11; Label G); appeared thickened (Figure 8.12b)

Table 8.4 illustrates a comparative summary of the medulla of the kidney of the control and aspartame treated rabbits to illustrate the possible effects of aspartame.

Table 8.5: Comparative summary of the medulla of the kidney of both the control and aspartame treated rabbits to illustrate the possible effects of aspartame

	Control rabbits	Aspartame treated rabbits
Simple cuboidal epithelium of proximal convoluted tubule		
Cellular membranes	Clearly visible (Fig. 8.13)	Damaged (Fig. 8.16)
Cytoplasm	Light pink with filament-like structures (Fig. 8.15a and 8.15b)	Transparent; Filament-like structures few to absent (Fig. 8.18a)
Nuclei	Round to oval (Fig. 8.15a and 8.15b)	Round to oval (Fig. 8.18a)
Simple squamous epithelium of the thin segment of the loop of Henle's		
Nuclei	Flattened and elongated (Fig. 8.15a and 8.15b)	More rounded (Fig. 8.17 and 8.18b)
Endothelial lining of the vasa recta		
Nuclei	Flattened, ovoid shape (Fig. 8.15c)	Round nucleus (Fig. 8.18b)

8.5 CONCLUSION

Blood circulated through both the liver and kidneys as to detoxify and to form urine respectively. It was seen in the previous chapters that the different components of blood was adversely affected by aspartame (leukocytes, coagulation factors, fibrin networks and platelet aggregation), thus it is hypothesized that the different filtering organs (liver and kidneys) might also be adversely affected.

8.5.1 Morphology of the liver

Damage to the cellular membranes were observed (Figure 8.3a) after treatment with aspartame and distinct changes were observed in the cytoplasm of the hepatocytes. The lace-like appearance of the cytoplasm changed to a spaced and broken appearance with the filament-like structures becoming less or was even absent (Figures 8.3a, 8.3b and 8.4a). The nuclei of the aspartame treated hepatocytes retained the scattered pattern of their chromatin granules, but their granules became more prominent with transparent areas becoming visible between the granules (Figure 8.4b). Three sections of the liver were studied: centre, left lobe and the right lobe. No differences was observed between the three sections in the control rabbits, but distinct differences were observed between the centre of the liver and left and right lobes of the liver respectively. It appeared as though the left and right lobes were not as severely affected by the treatment with aspartame as the centre of the liver. It is therefore hypothesized that the further the distance from the centre of the liver (main blood supply) the less the effects of aspartame on the liver.

A number of bi-nucleate hepatocytes were present in both the control (Figure 8.5) and aspartame treated liver (Figure 8.6). Literature indicates that up to 25 percent of hepatocytes in the liver could be bi-nucleate (Leeson *et al*., 1988a). It was determined that the control had 8.57% bi-nucleate hepatocytes and this value was set as the normal value. In total, 45 hepatocytes were counted (clearly visible nuclei) in the aspartame treated rabbit and 7 of the 45 hepatocytes were bi-nucleate. Thus, 8.57% of the 7 bi-nucleate hepatocytes in the aspartame treated rabbits were equal to four. Thus four of the seven hepatocytes were bi-nucleate, the other three hepatocytes were undergoing mitosis to repair the damaged caused by the aspartame as discussed above. In humans, if both factor VII and X are decreased, the individual suffers from prolonged hepatitis (Package insert – STA Deficient X; Ref 00738). Thus it is hypothesized that this was the case here after treatment with aspartame, as damage to the liver was histologically established, confirming why the concentration of both factors VII and X could be decreased (chapter 5). A possible explanation for why factors II, V and IX were not affected by the aspartame could not be determined, but further studies into this phenomenon should be undertaken.

The endothelial lining of the central vein (Figure 8.3b) was damaged, as the cells could not be distinguished. Factor VIII is secreted by vascular endothelium, thus this could be an indication as to why the levels of factor VIII were decreased. The damage to the endothelium in the liver together with the damage to the endothelium observed in the aorta (chapter 7) explains why the total concentration of circulating factor VIII was decreased (chapter 4). The subsequent damage to the liver could be the direct cause of the high level of circulating phenylalanine in the blood, resulting in a decreased amount of phenylalanine being converted to tyrosine via phenylalanine hydroxylase. Thus, phenylalanine is more likely to occupy the NAAT, inhibiting the transport of tryptophan (precursor for serotonin) over the BBB. Thus it is hypothesized that the damage can cause lowered level of serotonin, needed for optimal functioning of cAMP. Thus the damage to the liver could indirectly lead to the compromised BBB effect.

8.5.2 Morphology of the kidneys

Normal morphology of the renal corpuscle and urinary space were observed in the control rabbits in the cortex of the kidneys (Figure 8.7a and 8.7b; Figure 8.8). This changed however after treatment with aspartame. The urinary space of the renal corpuscle appeared enlarged (Figure 8.10) after treatment with aspartame. Erythrocytes were captures underneath the parietal layer of the capsule of Bowman (Figure 8.11, label E) which was not observed for the controls. The parietal layer of the capsule of Bowman also appeared thickened (Figure 8.12a). An increased number of mesangial cells were visible between the capillaries of the glomerulus (Figure 8.11; label C).

The most visible change caused by the aspartame was the appearance of a thickened visceral layer of the capsule of Bowman. The visceral layer of the capsule of Bowman closely invests the glomerular capillaries, with nuclei on the capsular side of the basal laminae of the capillaries, but the cells are greatly modified and do not form a complete sheet. The cells are called podocytes and are basically stellate in form, with their cell bodies rarely in contact with the basal lamina. The podocytes have a number of primary and secondary processes or pedicles. Pedicles of adjacent podocytes and podocytic processes interdigitate in a complex manner, often with the primary processes of one prodocyte overlying the primary processes and pedicles of a neighbouring podocyte. Between pedicles is an extensive system of clefts, or

intercellular spaces, known as filtration slits. This arrangement whereby much of the capsular surface of glomerular capillaries is covered by interdigitating pedicles between which are filtration slits, proves a large area for filtration, as all slits eventually drain to capsular space and thus into the lumen of the proximal convoluted tubule (Leeson *et al*., 1988b). Thus it is hypothesized that a thickened visceral layer, caused either by changes in the endothelium, basal lamina or the podocytes, will negatively influence the rate of filtration of blood to form the glomerular filtrate.

Normal morphology was observed for the cuboidal epithelium of the proximal convoluted tubule and the squamous epithelium of the thin segment of the loop of Henle in the control rabbit. The endothelial cells had their characteristic flattened, elongated nuclei. The cuboidal epithelial cells that line the proximal convoluted tubule have structural characteristics suitable for reabsorption (Kierszenbaum, 2002). Thus, if these cells are damaged, as were the case in this study (Figure 8.16 and 8.18a), reabsorption of fluid could be affected. The endothelial cell nuclei of the vasa recta were damaged, with the nuclei being more rounded (Figure 8.18b) than those observed in the controls, also indicating that aspartame affected the endothelial lining inside the medulla of the kidney.

It can therefore be concluded that aspartame negatively influenced the morphology of both the liver and the kidney. Damage to the liver was confirmed histologically, supplying evidence of the lowered concentrations of circulating factors VII and X (chapter 4).

The histology of the kidney was also affected by the aspartame, with major effects to the visceral layer of the capsule of Bowman and the cuboidal epithelium of the proximal convoluted tubule. It is suggested however, that further ultra-structural studies must be performed on the effects of aspartame on the renal corpuscle and cuboidal epithelium of the proximal convoluted tubule as they form key components of the urinary system.